Journal of Medicinal Chemistry

Article

pubs.acs.org/jmc

Discovery of Potent and Selective Pyrazolopyrimidine Janus Kinase 2 Inhibitors

Emily J. Hanan,[†] Anne van Abbema,[‡,#] Kathy Barrett,[‡] Wade S. Blair,[‡,¶] Jeff Blaney,[†] Christine Chang,[‡] Charles Eigenbrot,[§] Sean Flynn,[⊗] Paul Gibbons,[†] Christopher A. Hurley,[⊗] Jane R. Kenny,[∥] Janusz Kulagowski,[⊗] Leslie Lee,[⊥] Steven R. Magnuson,[†] Claire Morris,[⊗] Jeremy Murray,[§] Richard M. Pastor,[†] Tom Rawson,[†] Michael Siu,[†] Mark Ultsch,[§] Aihe Zhou,[†] Deepak Sampath,[⊥] and Joseph P. Lyssikatos*[,†]

[†]Departments of Discovery Chemistry, [‡]Biochemical and Cellular Pharmacology, [§]Structural Biology, [∥]Drug Metabolism and Pharmacokinetics, [⊥]Translational Oncology, Genentech, Inc. 1 DNA Way, South San Francisco, California 94080, United States

[⊗]Argenta, 8/9 Spire Green Centre, Flex Meadow, Harlow, Essex CM19 5TR, United Kingdom

Supporting Information

ABSTRACT: The discovery of somatic Jak2 mutations in patients with chronic myeloproliferative neoplasms has led to significant interest in discovering selective Jak2 inhibitors for use in treating these disorders. A high-throughput screening effort identified the pyrazolo[1,5-*a*]pyrimidine scaffold as a potent inhibitor of Jak2. Optimization of lead compounds **7a**−**b** and **8** in this chemical series for activity against Jak2, selectivity against other Jak family kinases, and good in vivo pharmacokinetic properties led to the discovery of **7j**. In a SET2 xenograft model that is dependent on Jak2 for growth, **7j** demonstrated a time-dependent knockdown of pSTAT5, a downstream target of Jak2.

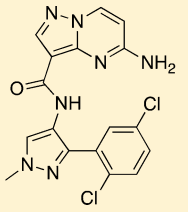

Compound **7j**
Jak2 K_i = 0.1 nM
pSTAT5 IC_{50} = 7.4 nM

INTRODUCTION

The Janus kinase (Jak) family consists of four nonreceptor tyrosine kinases (Jak1, Jak2, Jak3, and Tyk2) that play important roles in hematopoiesis and immune response.[1] Upon activation through cytokine signaling, Jaks subsequently activate the downstream signal transducer and activator of transcription (STAT) family of transcription factors, which regulate target gene expression that govern cell proliferation and survival.[2] The identification of a single gain of function point mutation in the JH2 pseudokinase autoinhibitory domain of Jak2 (Jak2^{V617F}), which renders the kinase constitutively active, has led to interest in Jak2 as a potential therapeutic target.[3]

Philadelphia (Ph)-negative myeloproliferative disorders (MPDs) are a group of heterogeneous hematologic diseases resulting from deregulated proliferation of differentiated myeloid cells and include the disorders polycythemia vera (PV), essential thrombocytemia (ET), and primary myelofibrosis (PMF).[4] Gain of function mutations in Jak2 are frequently observed in these disorders; the Jak2 mutation has been identified in 77% of patients with PV, in 35% of patients with ET, and 43% of patients with PMF.[5] In preclinical cellular models of PV, Jak2^{V617F} expression is necessary and sufficient to drive cytokine-independent activation of STAT1 or STAT5 and subsequently regulates cell proliferation and survival. Therefore, the identification of the Jak2^{V617F} somatic mutation provides a strong and compelling rationale to develop a targeted therapy for Ph-negative MPDs.

Indeed, a number of small molecule ATP-competitive Jak2 inhibitors are currently in clinical development for the treatment of MPDs, including TG101348,[6] SB1518,[7] AZD1480,[8] LY2784544,[9] and CYT387[10] (Figure 1). The recent FDA approval of ruxolitinib for the treatment of patients with intermediate or high-risk MF (including apMF, post-PV MF, and post-ET MF) has validated this target.[11] As a pan-Jak inhibitor, ruxolitinib has equivalent activity against Jak1 and Jak2, with decreased activity against Jak3 and Tyk2.[12] To potentially increase the safety index of a Jak2 inhibitor, it would be advantageous to identify a Jak2-selective inhibitor in light of the anticipated chronic dosing required for MPD treatment and the potential for immunosuppressive side effects related to inhibition of Jak1, Jak3, or Tyk2.[13,14] While the degree of selectivity for Jak2 over Jak1, Jak3, and Tyk2 necessary for therapeutic benefit is unclear, a 10-fold window would provide a minimum degree of differentiation. We therefore initiated a program to identify potent inhibitors of Jak2 with at least 10-fold selectivity against all other Jak family members.

The pyrazolo[1,5-*a*]pyrimidine scaffold was identified through high-throughput screening to have inhibitory activity against Jak2, and after initial medicinal chemistry exploration, compounds **7a**−**b** and **8** were identified as lead compounds with good inhibitory activity against Jak2 (Table 1). These compounds are close to the desired 10× selectivity against Jak1, with even better selectivity against the other Jak family

Received: August 22, 2012
Published: October 12, 2012

dx.doi.org/10.1021/jm3012239 | *J. Med. Chem.* 2012, 55, 10090−10107

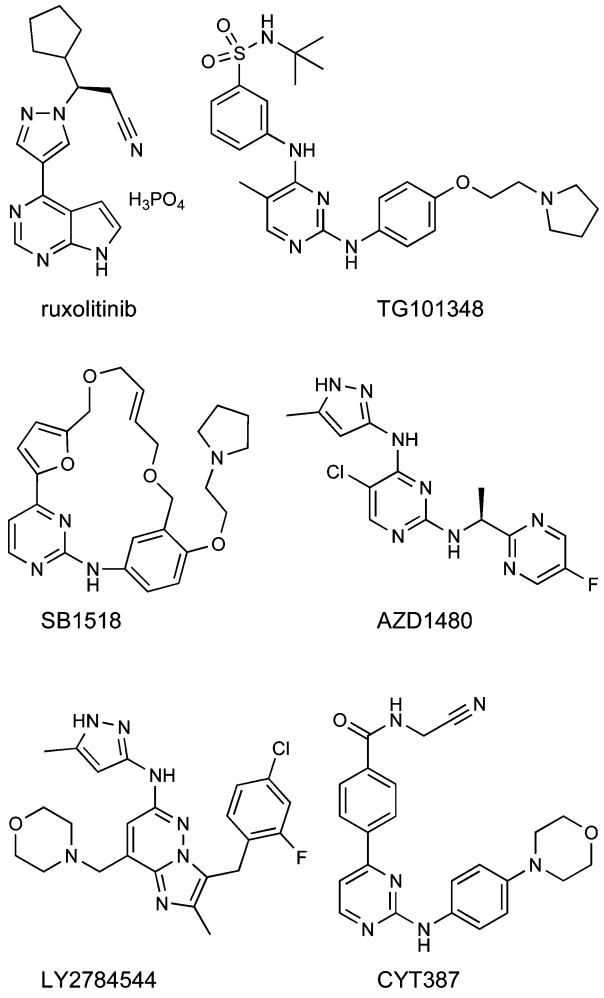

Figure 1. Examples of Jak2 inhibitors.

Table 1. Early Lead Inhibitors

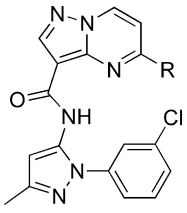

	NH_2 **7a**	$NHCH_3$ **7b**	H **8**
Jak2 K_i (nM)	2.5	5.1	11.9
LE[a]	0.46	0.43	0.44
LELP[b]	4.5	6.5	5.0
Jak1/2[c]	8.6	7.8	9.4
Jak3/2[c]	30.4	31.3	58.5
Tyk2/Jak2[c]	32.4	24.4	24.6
pSTAT5 IC_{50} (nM)[d]	131	259	1100
CYP450 inhibition IC_{50} (μM)[e]	>5	>10	4.6 (3A4)

[a]Ligand efficiency[15] (LE) calculated as ΔG (in kcal/mol) divided by the number of heavy atoms. [b]LELP[16] = cLogP[17]/LE. [c]fold biochemical selectivity for Jak2 over other Jak family kinase. [d]pSTAT5 SET2 MSD format. [e]CYP isoforms tested: 1A2, 2C9, 2C19, 2D6, 3A4; IC_{50} is given for most potently inhibited isoform.

members Jak3 and Tyk2. With these compounds as a starting point, we undertook a lead-optimization program to address the liabilities of **7a** and **8** and to identify a Jak2 inhibitor with an in vitro and in vivo profile suitable for the effective oral treatment of MPDs. The in vitro parameters measured for inhibitors synthesized as part of this lead-optimization campaign are provided in Tables 2−4, with in vivo pharmacokinetic parameters detailed in Table 5. This work culminated in the discovery and evaluation of **7j** as a potent and selective orally active inhibitor of Jak2.

CHEMISTRY

The general synthetic procedure for 5-aminopyrazolo[1,5-*a*]pyrimidine-3-carboxamides **7a−k** is described in Scheme 1. 3-Amino-pyrazole and 1,3-dimethyluracil were heated together with sodium ethoxide in ethanol to produce the cyclized pyrazolo[1,5-*a*]pyrimidine intermediate compound **1**. After neutralization with acetic acid, iodination with *N*-iodosuccinimide provided **3**. Palladium-catalyzed carbonylation and subsequent saponification yielded intermediate **4**. Alternatively, **4** could be generated in a one-step condensation of 5-amino-1*H*-pyrazole-4-carboxylic acid with 1,3-dimethyluracil.[18] Bis-chlorination of **4** with $POCl_3$ generated the key intermediate **5**, which was derivatized sequentially through amide formation followed by an S_NAr reaction with ammonia or methylamine to yield compounds **7a−k**.

5-*H*-Pyrazolo[1,5-*a*]pyrimidine-3-carboxamides **8**, **10a−c**, **12**, **13a−g**, and **14a−j** were prepared in one or two steps from pyrazolo[1,5-*a*]pyrimidine-3-carboxylic acid as described in Scheme 2. Pyridine containing compounds **10a−c** were prepared as described in Schemes 2 and 3. 5-Bromo-2-methylpyridine was oxidized with mCPBA to generate the *N*-oxide **15**, which was nitrated to provide compound **16**. Pyridine-*N*-oxide **16** was then reduced with $SnCl_2$ to yield 5-bromo-2-methylpyridin-4-amine **17**. The acid chloride of pyrazolo[1,5-*a*]pyrimidine-3-carboxylic acid was generated using oxalyl chloride and then used to acylate each of 2-bromo-pyridin-3-amine, 3-bromo-pyridine-4-amine, or **17** to provide bromo-pyridines **9a−c**. Suzuki coupling with 3-chlorophenyl boronic acid yielded compounds **10a−c**.[19]

Regioisomeric pyrazole compound **12** was prepared in two steps. Pyrazolo[1,5-*a*]pyrimidine-3-carboxylic acid was reacted with 4-bromo-1-methyl-1*H*-pyrazol-3-amine under standard HATU-mediated amide coupling conditions, followed by coupling with 3-chlorophenyl boronic acid under Suzuki conditions (Scheme 2).

3-Aryl-4-aminopyrazole intermediates used for the synthesis of compounds **13** and **14** were prepared as described in Schemes 4−6. In Scheme 4, various aryl-substituted α-bromoacetophenones were treated with potassium phthalimide or di-*tert*-butyl-iminodicarboxylate to generate α-amino-ketones **18a−d**. Treatment of these ketones with 1,1-dimethoxy-*N*,*N*-dimethylmethanamine (DMFDMA) at elevated temperatures provided intermediates **19a−d**, which were cyclized with either hydrazine or methylhydrazine to yield 1-*H*-4-aminopyrazoles or 1-methyl-1*H*-4-aminopyrazoles, respectively (**20a−e**).[20]

As an alternate preparation, as described in Scheme 5, acid chlorides or benzoic acids activated by CDI were treated with potassium ethyl malonate and $MgCl_2$ to provide β-keto-esters **21a−b**.[21] Reaction with DMFDMA gave **22a−b**. **22a** was cyclized with hydrazine to provide pyrazole **23**, which was alkylated with iodomethane to yield a regioisomeric mixture of pyrazoles **24a** and **25**. Carrying forward the regioisomeric mixture, saponification of the ester followed by Curtius rearrangement using Shioiri's conditions[22] to the *tert*-

dx.doi.org/10.1021/jm3012239 | J. Med. Chem. 2012, 55, 10090−10107

Scheme 1. General Synthetic Procedure for 5-Amino-pyrazolo[1,5-*a*]pyrimidine-3-carboxamides[a]

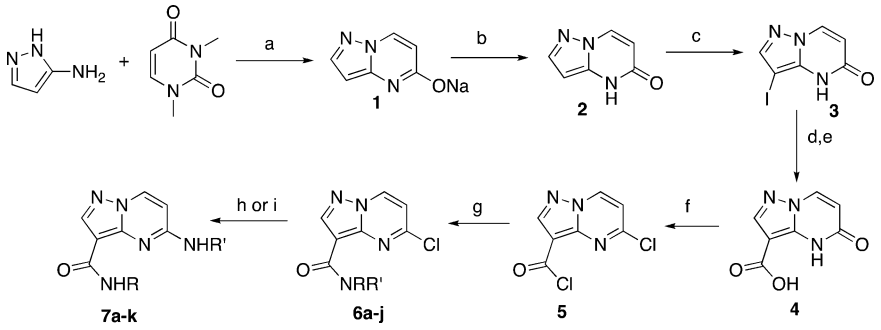

[a]Reaction conditions: (a) 21% EtONa, EtOH, 95%; (b) HOAc, H_2O, 85%; (c) *N*-iodosuccinimide, DMF, 86%; (d) CO (1 atm), $Pd(OAc)_2$, Et_3N, MeOH; (e) 5% aq LiOH, 68% (2 steps); (f) $POCl_3$, DIPEA, 87%; (g) H_2NR, DIPEA, DCM, 52−92%; (h) NH_3, iPrOH, DIPEA, μW 120 °C, 15 min, 9−80%; (i) H_2NCH_3, H_2O, μW 100 °C, 15 min, 62%.

Scheme 2. General Synthetic Procedure for Compounds 8−14[a]

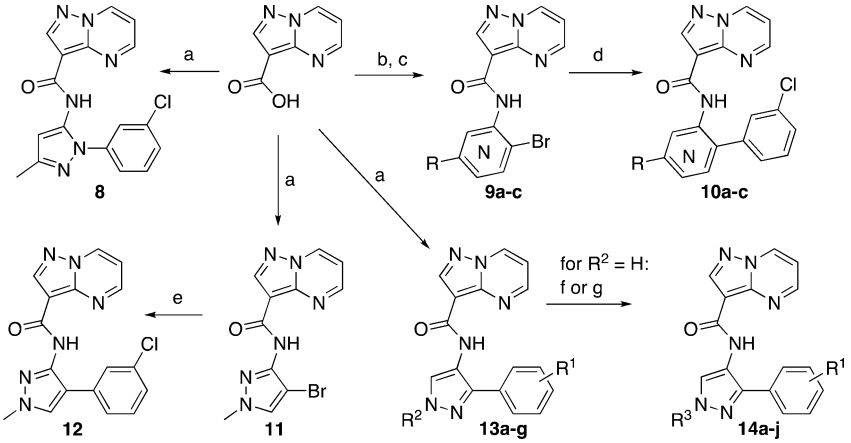

[a]Reaction conditions: (a) RNH_2, HATU or PyAOP, DIPEA, DMAP, 20−90%; (b) $(COCl)_2$, DCM; (c) 2-bromopyridin-3-amine or 3-bromopyridin-4-amine or **17**, Et_3N, DCM, 21−56%; (d) 3-chlorophenylboronic acid, $Pd(PPh_3)_2Cl_2$, Na_2CO_3, CH_3CN, H_2O, μW, 120 °C, 42−59%; (e) 3-chlorophenylboronic acid, $Pd(PPh_3)_4$, Na_2CO_3, diglyme, 100 °C, 7%; (f) R^3-X, Cs_2CO_3, DMF, 5−61%; (g) subsituted oxirane, Cs_2CO_3, DMF, 46%.

Scheme 3. Synthesis of Aminopyridine 17[a]

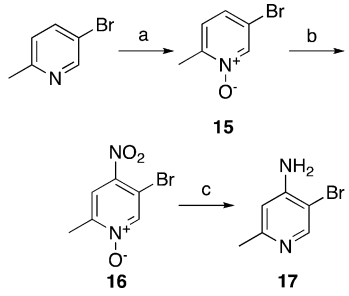

[a]Reaction conditions: (a) mCPBA, DCM, 99%; (b) HNO_3, H_2SO_4, 90%; (c) $SnCl_2$, HCl, 56%.

Scheme 4. 2-Bromo-1-phenylethanone-Based Synthesis of 1-Methyl-3-phenyl-1*H*-pyrazol-4-amines[a]

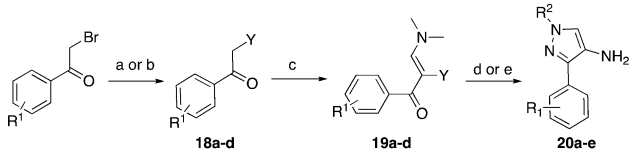

18a, 19a: R^1 = 3-Cl, Y = NPhth
18b, 19b: R^1 = 2,5-CH_3, Y = $NBoc_2$
18c, 19c: R^1 = 2,5-Cl, Y = $NBoc_2$
18d, 19d: R^1 = 2,5-Cl, Y = NPhth

20a: R^1 = 3-Cl, R^2 = Me
20b: R^1 = 3-Cl, R^2 = H
20c: R^1 = 2,5-CH_3, R^2 = H
20d: R^1 = 2,5-Cl, R^2 = H
20e: R^1 = 2,5-Cl, R^2 = Me

[a]Reaction conditions: (a) potassium phthalimide, 88%; (b) HN-$(Boc)_2$, NaH, 34−77%; (c) DMFDMA, 38−80%; (d) methylhydrazine, EtOH, 38−53%; (e) hydrazine, EtOH, 80%.

butylcarbamate and finally acid catalyzed Boc-deprotection yielded amino-pyrazoles **26a** and **27**, which are easily separated via silica gel chromatography.[23] Intermediate **22b** was reacted with *N*-methylhydrazine to give the desired regiosiomer **24b** directly, which was carried forward in the same manner to provide aminopyrazole **26b**.

The preferred construction of the 3-aryl-4-amino-pyrazole intermediate used for compound **14j** is described in Scheme 6. The SEM-protected 4-nitropyrazole **28** was subjected to palladium-catalyzed direct arylation conditions[24] with 2-bromo-4-chloro-1-methoxybenzene. The biaryl product **29** was then reduced with iron in the presence of ammonium chloride to yield SEM-protected 4-aminopyrazole **30**. Intermediate **30** was carried forward as described in Scheme 2, with SEM deprotection effected with aqueous HCl in ethanol, to provide the final compound **14j**.

dx.doi.org/10.1021/jm3012239 | *J. Med. Chem.* 2012, 55, 10090−10107

Scheme 5. Benzoic Acid Based Synthesis of 3-(5-Chloro-2-methylphenyl)-1-methyl-1*H*-pyrazol-4-amine[a]

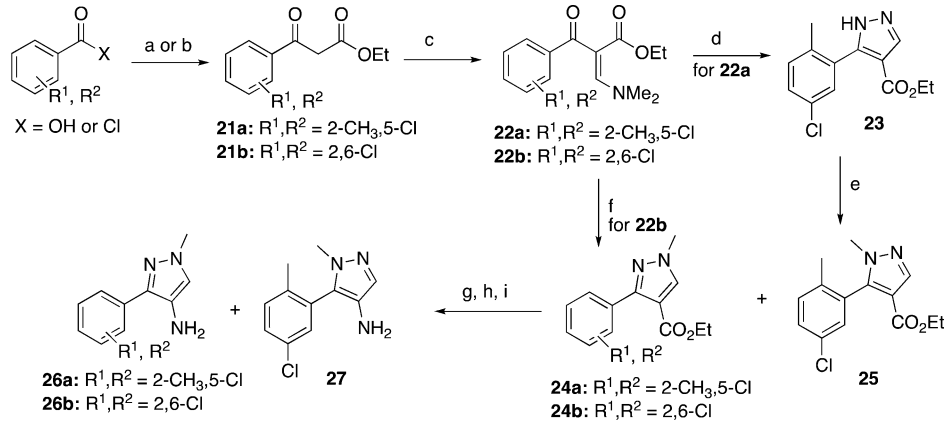

[a]Reaction conditions: (a) potassium ethyl malonate, CDI, $MgCl_2$, THF, 50 °C; (b) potassium ethyl malonate, Et_3N, $MgCl_2$, CH_3CN; (c) DMFDMA, 34−70% (2 steps); (d) hydrazine, EtOH, 70 °C, quant; (e) CH_3I, Cs_2CO_3, DMF, 40 °C, 81%; (f) methylhydrazine, AcOH, 45%; (g) NaOH, EtOH/H_2O; (h) $(PhO)_2P(O)N_3$, Et_3N, 1,4-dioxane, tBuOH; (i) HCl, 1,4-dioxane, 37−46% (3 steps).

Scheme 6. 4-Nitropyrazole CH-arylation Synthesis of 30[a]

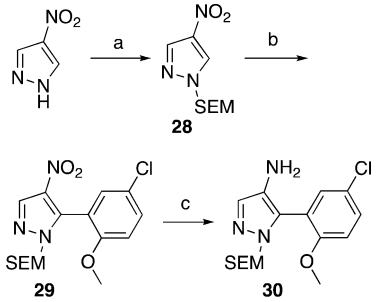

[a]Reaction conditions: (a) SEM-Cl, NaH, THF, 99%; (b) 2-bromo-4-chloro-1-methoxybenzene, $Pd(OAc)_2$, $(Ad)_2BuP$, K_2CO_3, $tBuCO_2H$, DMF, 120 °C, 89%; (c) Fe, NH_4Cl, EtOH, H_2O, 70 °C, quant.

Scheme 7. Synthesis of Aminoisoxazole 35[a]

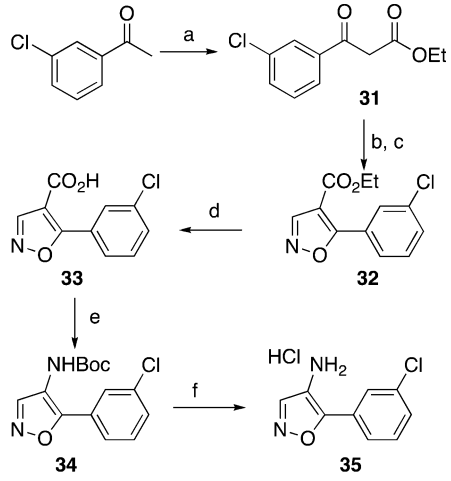

[a]Reaction conditions: (a) diethyl carbonate, NaH, toluene, rt to reflux, 51%; (b) DMFDMA, DMF, reflux; (c) NH_2OH-HCl, MeOH, reflux, 79% (2 steps); (d) HCl, AcOH, reflux; (e) $SOCl_2$, reflux, NaN_3, acetone, 0 °C to rt, tBuOH, 85 °C, 55% (2 steps); (f) 4 M HCl in 1,4-dioxane, 40 °C, quant.

The regioisomeric aminoisoxazole intermediates used for the preparation of compounds **7e** and **7f** were synthesized as described in Schemes 7 and 8. Acylation of 1-(3-chlorophenyl)-ethanone provided β-keto-ester **31**, which was reacted with DMFDMA and then cyclized to the isoxazole **32** using hydroxylamine. Hydrolysis of the ester followed by Curtius rearrangement yielded Boc-protected amine **34**, which was deprotected with HCl to give 5-(3-chlorophenyl)isoxazol-4-amine **35**. Compound **35** was carried forward as described in Scheme 1 to yield compound **7e**. As shown in Scheme 8, 3-chlorobenzaldehyde was condensed with hydroxylamine to give oxime **36**. Chlorination of **36** with *N*-chlorosuccinimide provided α-chlorobenzaldoxime **37**. After treatment with triethylamine, **37** underwent [3 + 2] dipolar cycloaddition with 3-pyrrolidin-1-yl-acrylic acid ethyl ester **38** via the in situ generated benzonitrile oxide to afford isoxazole **39**. Acid catalyzed hydrolysis of the ester followed by Curtius rearrangement to the *tert*-butylcarbamate **41** and subsequent Boc-deprotection yielded 3-(3-chlorophenyl)isoxazol-4-amine **42**, which was carried forward as described in Scheme 1 to provide compound **7f**.

The amino-thiazole intermediate used for compound **7g** was prepared as described in Scheme 9. Heating commercially available α-amino-(3-chlorophenyl)acetonitrile hydrochloride in the presence of elemental sulfur and acetaldehyde directly yielded aminothiazole **43**. Compound **43** was carried forward as described in Scheme 1 to provide compound **7g**.

RESULTS AND DISCUSSION

An HTS campaign identified the pyrazolo[1,5-*a*]pyrimidine **7a** as a compelling lead molecule for our selective Jak2 inhibitor program. Compound **7a** is a low nanomolar inhibitor of Jak2 (K_i = 2.5 nM) with high ligand efficiency[15] (LE = 0.46), low ligand-efficiency-dependent lipophilicity[16] (LELP = 4.5), and has potent inhibitory activity (IC_{50} = 131 nM) in a Jak2-driven SET2 cell-based assay as measured by the inhibition of pSTAT5, a downstream target of Jak2 (Table 1). Compound **7a** has low potential for reversible inhibition of the 5 major human CYP450 isoforms and good in vitro permeability. Compound **7a** has moderate selectivity (~9−30×) against the other Jak family members and excellent selectivity across a panel of 177 kinases.[25] Some of the liabilities of compound **7a** include low microsomal stability across five species and poor thermodynamic aqueous solubility (Table 5). The pharmaco-

dx.doi.org/10.1021/jm3012239 | J. Med. Chem. 2012, 55, 10090−10107

Scheme 8. Synthesis of Aminoisoxazole 42[a]

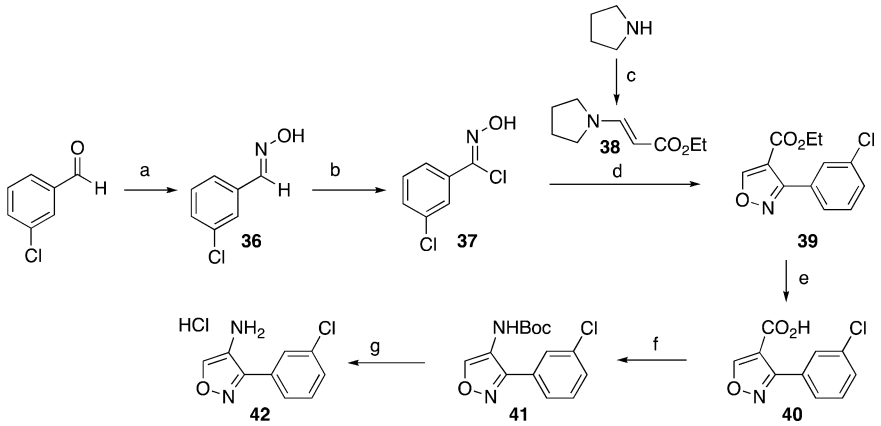

[a]Reaction conditions: (a) NH_2OH-HCl, pyridine, EtOH, quant; (b) NCS, DMF, quant; (c) ethyl propiolate, toluene, 94%; (d) Et_3N, Et_2O, 57%; (e) HCl, AcOH, reflux, 99%; (f) $(PhO)_2P(O)N_3$, Et_3N, tBuOH, 85 °C, 77%; (g) 4 M HCl in 1,4-dioxane, 97%.

Scheme 9. Synthesis of Aminothiazole 43[a]

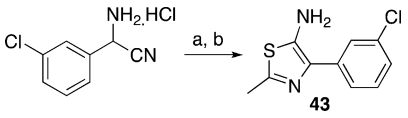

[a]Reaction conditions: (a) powdered sulfur, EtOH, 0 °C; (b) acetaldehyde, Et_3N, EtOH, 60 °C, 73% (2 steps).

kinetic profile of compound **7a** was determined for rats and mice[26] in order to determine how these apparent liabilities manifested in vivo (Table 5).

Compound **7a** has lower than expected plasma clearances in both mice and rats (3 and 6.8 mL/min/kg, respectively) because for both species microsomes predicted moderate/high clearance (Cl_{pred} = 60 and 39 mL/min/kg, respectively). The very low V_d in both species (V_{dss} = 0.27 and 0.19 L/kg, respectively) and lower than predicted plasma clearances are consistent with high plasma protein binding in both species (98.7% and 99.6%, respectively). Unfortunately, compound **7a** has poor oral bioavailability in mice and rats (F_{oral} (%) = 8.6 and 1, respectively). The limited oral exposure may be a result of poor aqueous solubility because the compound has good permeability. Moreover, the first pass effect should be minimal because the plasma clearance is low (Table 5).

We surmised that the poor solubility of **7a** was due to high crystal packing forces as a consequence of the multiple aromatic rings[27] (four) and multiple potential hydrogen bond donors (HBDs) and acceptors (HBAs). Poor aqueous solubility is also often associated with high lipophilicity; however, because the cLogP[17] of compound **7a** is in a reasonable range (2.1), lipophilicity may not be the key driver for the poor aqueous solubility. The rat pharmacokinetic profile of the 2-*des*-amino compound **8** and the 2-methylamino compound **7b** were obtained to probe the effect of removing HBDs on oral bioavailability (Table 5). The rat plasma clearance and V_d of compound **8** are low as was observed with compound **7a**; however, a much-improved oral exposure was observed (F_{oral} (%) = 44 vs 1). The improved oral exposure may be a result of the greater kinetic aqueous solubility of compound **8** vs **7a** because their thermodynamic solubilities, are comparable and both compounds have similar permeability in MDCK cells. Unfortunately, compound **8** is ∼10-fold less potent than compound **7a** against Jak2 in both the enzyme and cell assays. However, compound **7b**, in which the 2-NH_2 group is replaced with a 2-$NHCH_3$ group, was only 2-fold less potent in the Jak2 enzyme assay (K_i = 5.1 nM, Table 1). Compound **7b** unfortunately has high clearance in rats, which is consistent with the ∼4× higher free fraction in rat plasma (1.7% vs 0.4%) and higher predicted clearance in rat microsomes (48 vs 39 mL/min/kg) as compared to compound **7a**. Interestingly, compound **7b** has a significantly higher oral bioavailability compared to compound **7a** (F_{oral} (%) = 30 vs 1, Table 5) despite the higher plasma clearance. The improved oral exposure may be a result of the greater kinetic aqueous solubility of compound **7b**.

An X-ray structure of **8** with Jak2 was solved (Figure 2), revealing a binding mode consistent with observed SAR. The

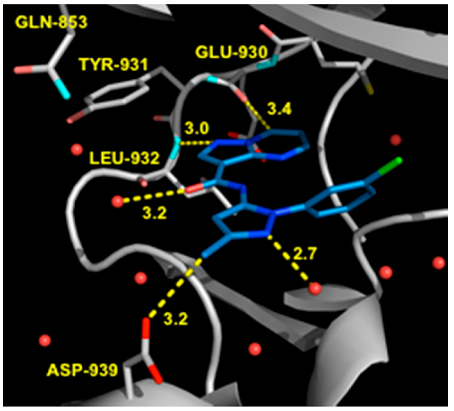

Figure 2. Co-crystal structure (2.3 Å) of compound **8** in the active site of the Jak2 kinase domain with the P-loop removed to allow a better view of the key active site interactions. Dashed lines indicate close contacts between ligand and protein with distances labeled in Å.

N1-nitrogen of the pyrazolopyrimidine core makes a hydrogen bond with the backbone NH of Leu932. A possible weak nonclassical hydrogen-bond between the C−H moiety at C-7 of the pyrazolopyrimidine core and the backbone of carbonyl Glu930 is interesting; however, the distance of this putative hydrogen bond is a bit long (3.4 Å).[28] Both the amide carbonyl and the pyrazole N2-nitrogen of **8** form hydrogen bonds to waters, and the terminal phenyl ring of **8** occupies the hydrophobic sugar region of the ATP binding site.

dx.doi.org/10.1021/jm3012239 | J. Med. Chem. 2012, 55, 10090−10107

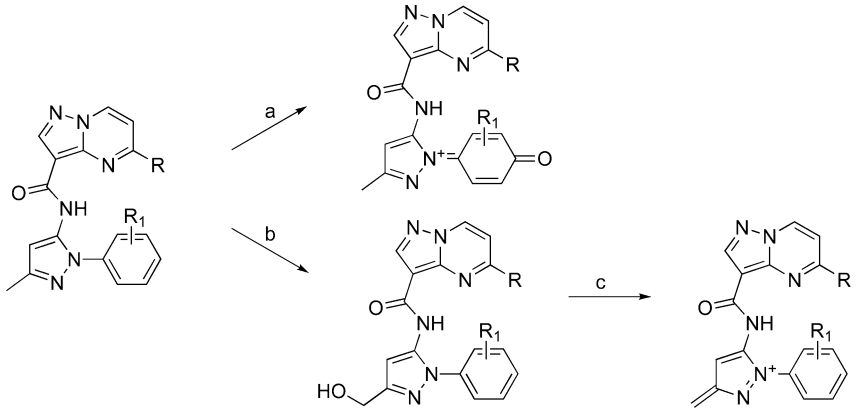

Figure 3. Potential reactive metabolites of the 3-methyl-*N*-aryl-methylpyrazole scaffold.

While a high degree of sequence homology exists between Jak1 and Jak2, several differences are observed in amino acids at the periphery of the binding site. The residue Asp939 in Jak2, which is in close proximity to the pyrazole methyl substituent, is Glu966 in Jak1. Other residue differences with the potential to interact with bound ATP-competitive ligands are Jak2 Tyr931→Jak1 Phe958 and Jak2 Gln853→Jak1 Arg879.[29] As these amino acids are somewhat removed from the space occupied by **8** and other compounds in this series, improvement of selectivity for Jak2 over Jak1 remained a challenging task, with the best potential for Jak1/Jak2 differentiation offered by positive interactions with Asp939.

In addition to the poor solubility and poor metabolic stability in human liver microsomes, we were also concerned about two potential reactive metabolites[30] of the 3-methyl-*N*-arylpyrazole core of the lead series as shown in Figure 3. The *N*-linked pyrazole moiety could potentially be oxidized to the para-quinoneimine (pathway A). Furthermore, the electron-rich nature of the aryl ring of the *N*-arylpyrazole moiety may contribute to the poor microsomal stability. The other potential reactive metabolite is envisioned to form through a two-step process in which the methyl group is oxidized to the alcohol, which subsequently eliminates to give the potentially highly reactive pyrazoleiminium species (Figure 3, pathway B and C). Therefore, in parallel with the efforts exploring the SAR of compound **7a**, a significant effort was expended to explore replacements for the *N*-arylpyrazole group.

The pyridine and regioisomeric pyrazole core replacements that were prepared are shown in Table 2. 4-Pyridyl **10b** is marginally more active than 3-pyridyl **10a**. Not surprisingly, 4-pyridyl **10b** exhibited potent CYP3A4 inhibition (IC_{50} = 0.2 μM), which is likely related to the heme-binding ability of a sterically unhindered pyridine nitrogen. Indeed, introducing a methyl substituent *ortho* to the pyridine nitrogen (compound **10c**) decreased CYP3A4 inhibition.[31] 4-Pyridyl compounds, **10b** and **10c**, have Jak family enzyme potencies similar to compound **8**.

Compound **13a** is the more potent of the regioisomeric pyrazoles (**12** and **13a**) that were prepared. The >30-fold decrease in the potency of **12** vs Jak2 as compared to **13a** may be ascribed to an increase in energy required to adopt a coplanar conformation between the amide and pyrazole groups due to lone pair repulsion between the *N*2 nitrogen of the pyrazole and one of the lone pairs of the amide oxygen. This is consistent with the binding mode for this scaffold observed in X-ray structures (e.g., Figure 2). Moreover, the pyrazole ring nitrogen of **13a** can form an H-bond to a water molecule consistently observed within the binding site, whereas regioisomer **12** is lacking a HBA at this position. Interestingly, **13a** is >2× more potent in both the Jak2 kinase and cell assays than **8** while maintaining moderate selectivity within the Jak family. The increase in potency may be due to an increase in the polarization of the C−H bonds of the *N*-methyl moiety of compound **13a** relative to the *C*-methyl group in compound **8**. As shown in Figure 2, a cocrystal structure of compound **8** with the Jak2 kinase domain indicated a potential charge-partial charge interaction (3.3 Å) of the carbonyl of Asp939 and the pyrazole methyl hydrogens. Presumably, this weak interaction could be enhanced with the increased polarization of the methyl protons in a pyrazole *N*-methyl group as compared to a *C*-linked methyl group. Although the methyl group of compound **8** is more acidic (calculated pK_a[32] 40 vs 43) due to resonance stabilization of the resulting anion into the pyrazole ring, the partial positive charge on the methyl protons are greater in compound **13a** due to greater polarization of the *N*-methyl bond. Compound **13a** has a similar rat plasma clearance to its regioisomer **8** (12.5 vs 13.3 mL/min/kg; Table 5). Interestingly, **13a** has high oral bioavailability despite poor kinetic and thermodynamic solubilities (both ∼1 μM). A possible explanation for the observed equivalence in kinetic and thermodynamic solubilities is that compound **13a** precipitated as a crystalline form during the kinetic solubility study.

To probe the putative pyrazole *N*-methyl effect further, **7c** was prepared in which the 5-*H* of the pyrazolopyrimidine ring was replaced with 5-NH_2 in an effort to improve Jak2 potency relative to **13a**. Gratifyingly, **7c** also has a >2-fold improvement in potencies in both in the Jak2 enzyme and cell assays as compared to its regioisomer **7a** (Table 2). Moreover, the selectivity against Jak1 is slightly increased. Unlike its regioisomer **7a**, the rat in vivo clearance of **7c** was well predicted by rat liver microsomes (Table 5). Although an improvement in oral bioavailability was observed with **7c** relative to **7a**, the oral bioavailability is still poor (7%). Assuming the observed plasma clearance is mainly hepatic-driven, the expected oral bioavailability is ∼60% (based on a hepatic extraction ratio of 0.40 and rat liver blood flow of 57 mL/min/kg) for a compound that is completely absorbed intact from the GI tract. As was observed with compound **7a**, compound **7c** has poor kinetic and thermodynamic aqueous solubility, which could explain the significantly lower than expected oral exposure (Table 5).

dx.doi.org/10.1021/jm3012239 | *J. Med. Chem.* 2012, 55, 10090−10107

Table 2. Pyrazole Replacement SAR

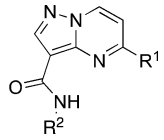

Compound	R^1	R^2	Jak2 K_i (nM)	Jak1/2[a]	Jak3/2[a]	Tyk2/ Jak2[a]	pSTAT5 IC_{50} (nM)[b]	CYP450 IC_{50} (μM)[c]
10a	H	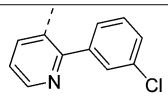	15.5	8.8	42.6	15.0	N.D.	>10
10b	H	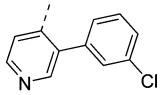	7.1	11.4	26.0	11.7	250	0.2 (3A4)
10c	H	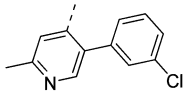	9.7	6.4	29.5	14.3	1100	>10
12	H	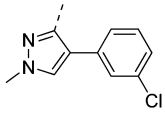	103	4.5	N.D.[d]	6.3	N.D.	>10
13a	H	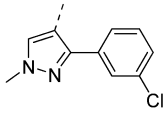	3.2	8.1	36.5	18.3	89.8	>10
13b	H	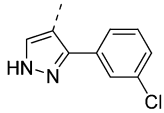	3.2	7.9	58.7	8.3	143	7.2 (3A4)
7c	NH_2	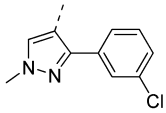	1.0	10.6	15.4	27.6	30.4	>10
7d	NH_2	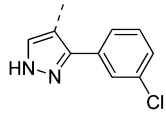	1.3	11.8	29.0	13.7	205	3.1 (1A2)
7e	NH_2	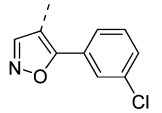	31.9	24.1	129	20.2	N.D.	0.5 (1A2)
7f	NH_2	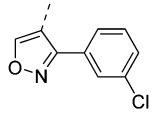	1.8	13.6	36.1	16.5	158	1.2 (1A2)
7g	NH_2	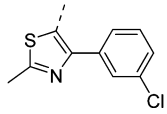	1.0	12.7	31.8	36.8	176	6.7 (3A4)

[a]Fold biochemical selectivity for Jak2 over other Jak family kinase. [b]pSTAT5 SET2 MSD format. [c]CYP isoforms tested: 1A2, 2C9, 2C19, 2D6, 3A4; IC_{50} is given for most potently inhibited isoform; [d]N.D.: not determined.

Two common strategies to improve stability toward CYP-mediated metabolism are to increase polarity and to remove and/or block metabolic hotspots such as *N*-methyl groups;[33] therefore, several compounds that lacked the *N*-methyl group were prepared. 1-*H*-Pyrazoles **7d** and **13b** have very similar Jak2 enzyme potencies relative to their corresponding *N*-methyl-1*H*-pyrazole analogs while preserving selectivity versus the other Jak family members (Table 2). Interestingly,

dx.doi.org/10.1021/jm3012239 | J. Med. Chem. 2012, 55, 10090−10107

Table 3. Pyrazole *N*-Substitutions

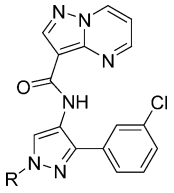

Compound	R	Jak2 K_i (nM)	Jak1/2[a]	Jak3/2[a]	Tyk2/Jak2[a]	Kinetic solubility pH 7.4 (μM)	HLM, RLM Cl_{pred} (mL/min/kg)
13a		3.2	8.1	36.5	18.3	1	18, 36
14a		49.0	2.7	47.1	8.8	44	6.7, 26
14b	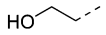	5.6	7	39.7	9.6	22	17, 30
14c	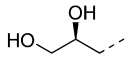	14.0	7.7	43.3	19.4	>200	13, 19
14d	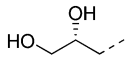	41.1	5.3	26	13.5	>200	12, 27
14e	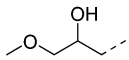	16.7	4.1	49.8	16.2	102	15, 32
14f	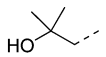	41.2	1.5	58.6	14.9	37	7.8, 18
14g	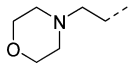	63.3	1.8	24.9	12.2	<1	20, 47

[a]Fold biochemical selectivity for Jak2 over other Jak family kinase.

compound **7d** is ~7× less potent than *N*-methyl analog **7c** in the Jak2 cell assay. Unfortunately, removing the *N*-methyl moiety coupled with an increase in polarity did not lead to improved human liver microsome (HLM) stability. Because the pyrazole core may be the key metabolic liability in this series, two isomeric isoxazoles (**7e–f**) and a methylthiazole (**7g**) were prepared. All three compounds have a heteroatom (O or N) *ortho* to the phenyl ring with a potential to form an H-bond with an active site water molecule. Isoxazole **7f** has comparable Jak2 kinase potency and Jak family selectivity to compounds **7c–d**. Interestingly, isoxazole **7e** is less potent against all Jak family members than its regioisomer **7f**. This may be a result of the poor H-bond accepting character of oxygen atoms in heteroaromatic ring systems, whereas sp^2 nitrogens of heteroaromatics tend to be good H-bond acceptors.[34] While the Jak2 activity of **7f** compared favorably with **13a**, it unfortunately potently inhibited CYP1A2 (IC_{50} = 1.2 μM). Finally, because 2-*H* thiazoles are generally potent CYP inhibitors,[35] we only prepared the 2-methyl-thiazole **7g** to mitigate this known risk. This particular regioisomeric thiazole was chosen because it was presumed that an attractive intramolecular thiocarbonyl interaction would stabilize the requisite coplanar geometry between the amide and five-membered heteroaryl required for potent Jak2 activity.[36] Compound **7g** was determined to be equipotent with compound **7c** in the Jak2 enzyme assay and slightly more selective vs the other Jak family members. It is, however, less potent in the Jak2 cell assay (K_i = 176 nM vs 60.4 nM). Moreover, compound **7g** is a moderate inhibitor of CYP3A4 (IC_{50} = 6.7 μM), whereas compound **7c** is inactive against all 5 CYP isoforms tested.

As part of our efforts to improve the aqueous solubility and metabolic stability of our lead series, various branched and hydrophilic substituents were prepared off the pyrazole nitrogen because this vector points toward bulk solvent (Table 3). These substituents are also in the region of the Jak2 Asp939→Jak1 Glu966 amino acid difference with the potential to impact selectivity over Jak1. The isopropyl-substituted compound **14a** was designed to increase the percentage of sp^3 centers, which has been correlated in the literature with improved solubility.[37] Moreover, by replacing the *N*-methyl group with an *N*-isopropyl, it was hoped that the metabolic stability might improve. Gratifyingly, **14a** is indeed more soluble than **13a** (44 μM vs 1 μM kinetic aqueous solubility) and more stable in HLMs; however, **14a** has poor Jak2 potency and selectivity vs Jak1 is eroded. The traditional method to improve aqueous solubility is to add hydrophilic groups such as hydroxyls or groups that are charged at physiological pH. Furthermore, increasing polarity often leads to an increase in metabolic stability toward CYP-mediated metabolism. The introduction of a single hydroxyl functional group (**14b**, **14e**, and **14f**) improved kinetic solubility significantly vs **13a** although only the *tert*-butyl alcohol analog **14f** showed a significant improvement in HLM stability (CL_{pred} = 7.8 vs 18 mL/min/kg). The greatest improvement in kinetic aqueous solubility was seen with the bis-hydroxy compounds **14c** and **14d**, both of which have measured kinetic aqueous solubilities >200 μM at pH 7.4. Moreover, both of these analogs are also more stable in HLMs than **13a**, although to a

dx.doi.org/10.1021/jm3012239 | J. Med. Chem. 2012, 55, 10090–10107

Table 4. Phenyl Bis-substitution SAR

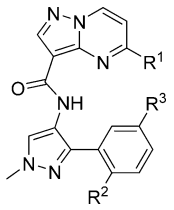

compd	R^1	R^2	R^3	Jak2 K_i (nM)	Jak 1/2[a]	Jak 3/2[a]	Tyk2/Jak2[a]	pSTAT5 IC_{50} (nM)[b]	HLM, RLM Cl_{pred} (mL/min/kg)	kinetic solubility pH 7.4 (μM)
14h	H	CH_3	CH_3	2.1	5.0	17.0	12.0	64.2	14, 42	9
14i	H	Cl	Cl	0.4	6.9	12.6	14.2	42.3	12, 11	6
13e	H	CH_3	Cl	0.6	4.4	19.4	7.4	34.5	17, 38	1
14j	H	OCH_3	Cl	0.3	1.7	25	5.1	22.4	13, 25	82
13g	H		2,6-Cl	5.2	10.4	2.1	39.6	242	7, 11	5
7h	NH_2	CH_3	H	1.6	6.0	3.2	14.6	68.6	11, 22	7
7i	NH_2	CH_3	CH_3	0.3	9.7	9.8	24.5	40.4	16, 36	6
7j	NH_2	Cl	Cl	0.1	14.8	9.7	43.7	7.4	14, 31	4
7k	NH_2	CH_3	Cl	0.1	9.2	13.1	20.1	9.8	15, 21	7

[a]Fold biochemical selectivity for Jak2 over other Jak family kinase. [b]pSTAT5 TF1+EPO MSD format.[38]

Table 5. Physicochemical/Pharmacokinetic[a] Parameters

	7a	7b	7c	7j	8	13a
solubility, pH 6.5 (μM)	2.7	<2.0	5.4	<2.0	5.7	<2.0
kinetic solubility, pH 7.4 (μM)	7	121	44	4	>200	1
%PPB (human, rat)	99.5, 99.6	98.4, 98.3	98.9, 99.7	98.5, 98.5	95.8, 99.3	99.4, 99.7
MDCK A-B $10E^{-6}$ cm/sec (B-A/A-B)	8.4 (1.3)	15.1 (0.9)	ND[b]	10.5 (0.7)	10.5 (0.5)	ND
HLM_{CL}, RLM_{CL} (mL/min/kg)	15, 39	17, 48	15, 23	14, 31	18, 36	18, 36
CL_p (iv, mL/min/kg)	6.8	51.3	23.1	12.6	13.3	12.5
Vd_{ss} (iv, L/kg)	0.185	0.843	0.355	1.08	0.293	0.349
$T_{1/2}$ (iv, hr)	0.38	0.24	0.22	1.20	0.36	0.23
F_{oral} (%)	1	30	7	63	44	124

[a]Male Sprague–Dawley rats, 0.1–1 mg/kg iv (solution in 60% aqueous PEG 400); 5 mg/kg PO (suspension in 60% aqueous PEG 400). [b]ND = low recovery, permeability not calculated.

lesser extent than **14f**. Interestingly, the morpholino-containing compound **14g** has very poor kinetic aqueous solubility (<1 μM at pH = 7.4) and is highly unstable in HLMs. The poor solubility of **14g** may be due to the possibility that the morpholine group of **14g** is only partially protonated at pH = 7.4 (calculated pK_a = 7.06). Because all but one of these analogs are significantly less potent vs Jak2 than **13a**, coupled with the erosion of selectivity vs Jak1 with several of the compounds (**14a**, **14f** and **14g**), this subseries was not progressed further. Only the *N*-ethanol analog **14b** maintained good Jak2 potency and moderate selectivity vs Jak1; however, it has poor stability in HLMs. It is not clear as to why Jak2 activity dropped off significantly with most of these analogs given that these substituents seemingly point toward solvent. One possibility is that the side chain of the solvent-exposed Asp939 is less flexible than presumed, leading to steric clashes with groups larger than methyl substituted off the pyrazole.

We then focused efforts on optimizing the substituents of the phenyl ring. Parallel work (not shown) on the regioisomeric *N*-arylpyrazole series exemplified by compound **7a** indicated that any substitution at the *para*-position of the *N*-aryl group significantly decreases inhibitory potencies for all Jak family members. This observation is consistent with the binding mode observed for **8** (Figure 2, Supporting Information Figure S1) with the *para*-position of the phenyl ring abutting the back of the pocket. The preferred substituents in the 3-position are methyl, chloro, and cyano. Groups larger than chloro are not well tolerated. The X-ray cocrystal structure of **8** with Jak2 (Figure 2) suggests that there is hydrophobic space at both the top and bottom of the sugar-binding pocket within the ATP binding site. This led us to make directed bis-substitutions around the phenyl ring (Table 4). *ortho*-Substitution was designed to enforce a high degree of twist between the phenyl and pyrazole rings, thereby lowering the ground-state energy of the active conformation adopted in cocrystal structures, as well as decreasing the flatness of the compounds, which could improve solubility. The 2,5-dimethylphenyl compound **14h** is slightly more potent than **13a**; however, the 2,5-dichlorophenyl analog **14i** is nearly 10-fold more active with a K_i of 0.4 nM. The K_i of the 2-methyl-5-chlorophenyl analog **13e** is in-between that of **14h** and **14i**, which is consistent with the SAR. The 2,6-dichlorophenyl analog **13g** is nearly 10-fold less active against Jak2 than the corresponding 2,5-dichlorophenyl analog **14i**, with similar drops in activity against the other Jak family members. Compounds **14h–j** and **13e** spanned a ~3-fold range of activity in the Jak2 cell assay, with 2-chloro, 2-methyl, or 2-methoxy substituents resulting in similar activities. 2,5-Bis-substitution proved to be critical for optimal activity against Jak2 because the 2-monosubstituted analog **7h** and the 2,6-dichloro bis-substituted analog **13g** are 5–10× less potent than

dx.doi.org/10.1021/jm3012239 | J. Med. Chem. 2012, 55, 10090–10107

their respective 2,5-bis-substituted analogs **7i** and **14i**. Interestingly, only analogs **7i–k**, where $R^1 = NH_2$ in the 2,5-bis-substituted series are both highly potent vs Jak2 (K_i < 1nM) and also meet our selectivity requirements vs the other Jak family members (>10×).

On the basis of its Jak2 activity and selectivity, compound **7j** was dosed in rat pharmacokinetic studies (Table 5). Compound **7j** has good oral bioavailability (F_{oral} (%) = 63) despite poor kinetic and thermodynamic aqueous solubilities. The good oral exposure may be a result of the combination of low plasma clearance and high permeability. The low clearance was not unexpected given the predicted clearance based on rat microsomes coupled with high rat plasma protein binding. No reversible CYP inhibition was observed for the five major isoforms and only minimal time-dependent inhibition (TDI) of CYP3A4 (TDI IC_{50} = 5.8 μM with a 38% shift in AUC).[39] Compound **7j** is very selective against a panel of 183 kinases; when tested at 0.01 μM (100× the Jak2 K_i), **7j** inhibited only five kinases outside of the Jak family at >50%.[40]

The excellent oral exposure of **7j** in rats coupled with its potent Jak2 inhibition in cells prompted us to test whether it could knockdown Jak2-mediated phosphorylation of STAT5 in a SCID mouse SET2 xenograft model that is dependent on Jak2 for growth. At an oral dose of 100 mg/kg, 64% inhibition of pSTAT5 was observed at the 1 h time point, while the inhibition of pSTAT5 decreased as the plasma levels of **7j** decreased over time (Figure 4). A more in-depth discussion of the in vivo profile of **7j** has been published elsewhere including efficacy studies in preclinical PV and AML models.[41]

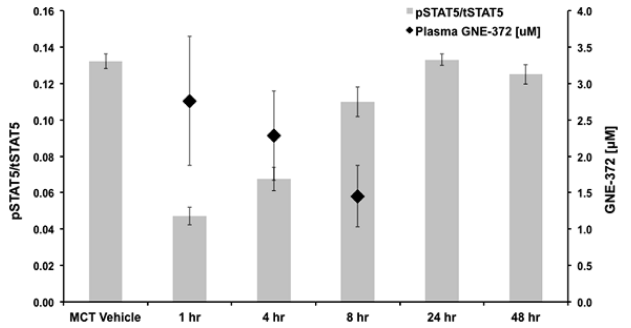

Figure 4. PK/PD study of **7j** at an oral dose of 100 mg/kg in a SET2 xenograft model.

CONCLUSIONS

In conclusion, a series of highly potent and selective novel pyrazolo[1,5-*a*]pyrimidine-based Jak2 inhibitors has been discovered. Optimization of lead compounds **7a–b** and **8** for potency and pharmacokinetic properties led to the discovery of **7j**, a potent Jak2 inhibitor (K_i = 0.10 nM) with high LE (0.49) and low LELP (5.9). Compound **7j** displays an adequate combination of cell potency, oral exposure, and in vivo knockdown of pSTAT5 making it a reasonable tool for proof of principal Jak2-dependent efficacy studies. Preclinical efficacy studies of **7j** in PV and acute myeloid leukemia (AML) models have been disclosed elsewhere.[41]

EXPERIMENTAL SECTION

General Methods. Unless otherwise noted, all solvents and reagents were obtained from commercial suppliers and used without further purification. Anhydrous solvents were obtained from EMD or Aldrich and used directly. All reactions involving air- or moisture-sensitive reagents were performed under a nitrogen atmosphere. Unless otherwise stated, operations were carried out at ambient temperature (in the range 18–25 °C). Microwave experiments were carried out using a Biotage Initiator 60, which uses a single-mode resonator and dynamic field tuning. Silica gel chromatography was performed using medium-pressure liquid chromatography on a CombiFlash Companion (Teledyne Isco) with RediSep normal-phase silica gel columns. All final compounds were purified to ≥95% as determined by an Agilent 1100 series HPLC using an Agilent ZORBAX SB-C18 30 mm × 2.1 mm column, eluting with a binary solvent system A and B using a gradient elusion [A, H_2O with 0.05% trifluoroacetic acid (TFA); B, CH_3CN with 0.05% TFA] with UV detection at 254 nm. ^{1}H NMR spectra were recorded on a Bruker 400 or 300 MHz NMR spectrometer using the deuterated solvent stated. Chemical shifts are reported in ppm from the solvent resonance. NMR data are reported as follows: chemical shift, multiplicity (s, singlet; d, doublet; t, triplet; q, quartet; m, multiplet; and br, broad peak), coupling constants, and number of protons. Mass spectral (MS) data was determined with a Sciex API150ex or Agilent 6140 spectrometer and ESI source.

*Sodium Pyrazolo[1,5-a]pyrimidin-5-olate (**1**).* A mechanically stirred mixture of 3-aminopyrazole (9.38 g, 113 mmol), 1,3-dimethyluracil (14.7 g, 105 mmol), and 21% sodium ethoxide in ethanol (170 mL) was heated to reflux for one h. The reaction mixture was cooled, filtered, and the collected solid washed with cold ethanol and vacuum-dried to yield 13.47 g (95%) of sodium pyrazolo[1,5-*a*]pyrimidin-5-olate. ^{1}H NMR (400 MHz, DMSO-d_6) δ: 8.0 (d, 1H), 7.43 (d, 1H), 5.65 (d, 1H), 5.37 (d, 1H). MS: *m*/*z* 136.0 ([M + H]$^+$).

*Pyrazolo[1,5-a]pyrimidin-5(4H)-one (**2**).* To **1** (13.47 g, 85.74 mmol) was added 500 mL of acetic acid and 100 mL of water. The mixture was stirred at ambient temperature for 15 min and then evaporated to dryness under vacuum. The residue was suspended in 300 mL of 9:1 dichloromethane (DCM):methanol and vacuum filtered through silica gel to remove sodium acetate. The silica gel pad was washed with 700 mL of additional 9:1 DCM:methanol solution. The combined DCM:methanol solution was concentrated to dryness. The solid product was suspended in 1:1 hexane:DCM and filtered to yield 9.9 g (85%) of pyrazolo[1,5-*a*]pyrimidin-5(4*H*)-one. ^{1}H NMR (400 MHz, DMSO-d_6) δ: 12.1 (br s, 1H), 8.47 (d, *J* = 7.9 Hz, 1H), 7.75 (d, *J* = 1.9 Hz, 1H), 5.94 (d, *J* = 7.5 Hz, 1H), 5.81 (d, *J* = 1.7 Hz, 1H). MS: *m*/*z* 136.0 ([M + H]$^+$).

*3-Iodopyrazolo[1,5-a]pyrimidin-5(4H)-one (**3**).* A mixture of **2** (1.0 g, 7.4 mmol) and *N*-iodosuccinimide (1.67 g, 7.42 mmol) was combined with 20 mL of DMF and warmed slightly until a heavy precipitate formed. The reaction mixture was stirred an additional 1 h at ambient temperature and then cooled on an ice–water bath and filtered. The collected solid was washed with 20 mL of DCM and air-dried to give 1.66 g (86%) of 3-iodopyrazolo[1,5-*a*]pyrimidin-5(4*H*)-one. ^{1}H NMR (400 MHz, DMSO-d_6) δ: 12.1 (s, 1H), 8.5 (d, *J* = 7.6 Hz, 1H), 7.84 (s, 1H), 6.01 (d, *J* = 7.1 Hz, 1H). MS: *m*/*z* 262.2 ([M + H]$^+$).

*5-Oxo-4,5-dihydropyrazolo[1,5-a]-pyrimidine-3-carboxylic Acid (**4**).* A mixture of **3** (1.5 g, 5.8 mmol), palladium(II) acetate (0.27 g, 1.2 mmol), triethylamine (2.3 mL, 17 mmol), and 75 mL of methanol was stirred, degassed with nitrogen twice under vacuum, and then blanketed with carbon monoxide under a balloon. The reaction mixture was heated to 55 °C for 5 h and then filtered through Celite and concentrated under vacuum. The residue was recrystallized from water and filtered to give 0.81 g (73%) of methyl 5-oxo-4,5-dihydropyrazolo[1,5-*a*]-pyrimidine-3-carboxylate. ^{1}H NMR (400 MHz, DMSO-d_6) δ: 11.0 (br s, 1H), 8.58 (d, *J* = 7.9 Hz, 1H), 8.19 (s, 1H), 6.19 (d, *J* = 7.9 Hz, 1H), 3.80 (s, 3H). A solution of methyl 5-oxo-4,5-dihydropyrazolo[1,5-*a*]-pyrimidine-3-carboxylate (0.75 g, 3.9 mmol), lithium hydroxide (0.466 g, 19.5 mmol), and 20 mL of water was stirred at ambient temperature for 3 h. Acetic acid (5 mL) was added to the reaction mixture, and the precipitated solid was collected by vacuum filtration to give 0.65 g (93%) of 5-oxo-4,5-dihydropyrazolo[1,5-*a*]pyrimidine-3-carboxylic acid. ^{1}H NMR (400

dx.doi.org/10.1021/jm3012239 | J. Med. Chem. 2012, 55, 10090–10107

MHz, DMSO-d_6) δ: 8.54 (d, J = 9.2 Hz, 1H), 8.06 (s, 1H), 6.11 (d, J = 7.2 Hz, 1H).

As an alternative preparation, to a stirred solution of 5-amino-1*H*-pyrazole-4-carboxylic acid (10.0 g, 71.4 mmol) in ethanol (100 mL) was added sodium ethoxide (17.0 g, 245 mmol) followed by 1,3-dimethyluracil (11.0 g, 78.6 mmol). The reaction mixture was then stirred at reflux under an argon atmosphere overnight. The mixture was poured into ice−water and concentrated HCl added to adjust the pH to ∼3−4. The mixture was stirred for 2 h, and the resulting precipitate was collected via filtration and dried under vacuum to yield 10.0 g (58%) of 5-oxo-4,5-dihydropyrazolo[1,5-*a*]pyrimidine-3-carboxylic acid. ^{1}H NMR (400 MHz, DMSO-d_6) δ: 8.54 (d, J = 9.2 Hz, 1H), 8.06 (s, 1H), 6.11 (d, J = 7.2 Hz, 1H).

*5-Chloropyrazolo[1,5-a]pyrimidine-3-carbonyl Chloride (**5**).* A mixture of **4** (0.371 g, 2.07 mmol), phosphorus oxychloride (20 mL), and DIPEA (1.2 mL, 6.9 mmol) was refluxed for 2 h. The reaction mixture was cooled and concentrated under reduced pressure. The residue was taken up in DCM and concentrated again 3 times. The residue was partitioned between water and DCM, and the DCM layer was dried with sodium sulfate, vacuum filtered through a bed of silica gel, and concentrated to give 390 mg (87%) of 5-chloropyrazolo-[1,5-*a*]pyrimidine-3-carbonyl chloride as a yellow solid which was used immediately without further purification. ^{1}H NMR (400 MHz, $CDCl_3$) δ: 8.72 (d, J = 7.2 Hz, 1H), 8.65 (s, 1H), 7.17 (d, J = 7.6 Hz, 1H).

*5-Chloro-N-(1-(3-chlorophenyl)-3-methyl-1H-pyrazol-5-yl)-pyrazolo[1,5-a]pyrimidine-3-carboxamide (**6a**).* A solution of **5** (150 mg, 0.694 mmol), 1-(3-chlorophenyl)-3-methyl-1*H*-pyrazol-5-amine (140 mg, 0.674 mmol), DIPEA (0.18 mL, 1.0 mmol), and 15 mL of DCM was stirred at ambient temperature for 3 days. The reaction mixture was partitioned between DCM and water, and the DCM phase was dried over sodium sulfate and vacuum filtered through a pad of silica gel. The silica gel pad was washed with 95:5 DCM:methanol. The combined filtrates were concentrated to give 250 mg (93%, 74% purity by HPLC) of 5-chloro-*N*-(1-(3-chlorophenyl)-3-methyl-1*H*-pyrazol-5-yl)pyrazolo[1,5-*a*]pyrimidine-3-carboxamide which was used without further purification. MS: m/z 387.2 ([M + H]$^+$).

*5-Amino-N-(1-(3-chlorophenyl)-3-methyl-1H-pyrazol-5-yl)-pyrazolo[1,5-a]pyrimidine-3-carboxamide (**7a**).* A mixture of 74% pure **6a** (55.0 mg, 1.05 mmol) and 3 mL of concentrated ammonium hydroxide was sealed and heated in a microwave reactor at 105 °C for 30 min. The reaction mixture was cooled, and the resulting precipitate was collected by filtration, rinsed with water, and dried under vacuum to yield 25.0 mg (48%) of 5-amino-*N*-(1-(3-chlorophenyl)-3-methyl-1*H*-pyrazol-5-yl)pyrazolo[1,5-*a*]pyrimidine-3-carboxamide, which was purified by reverse-phase HPLC and lyophilized. ^{1}H NMR (400 MHz, DMSO-d_6) δ: 9.93 (s, 1H), 8.65 (d, J = 7.5 Hz, 1H), 8.19 (s, 1H), 7.69−7.64 (m, 1H), 7.59 (d, J = 8.0 Hz, 1H), 7.51 (t, J = 8.0 Hz, 1H), 7.43 (d, J = 8.0 Hz, 1H), 6.42−6.37 (m, 2H), 2.24 (s, 3H). MS: m/z 368.3 ([M + H]$^+$).

*N-(1-(3-Chlorophenyl)-3-methyl-1H-pyrazol-5-yl)-5-(methylamino)pyrazolo[1,5-a]pyrimidine-3-carboxamide (**7b**).* A mixture of **6a** (172 mg, 0.444 mmol) and a 40 wt % solution of methylamine in water (3 mL, 4.44 mmol) was sealed and heated in a microwave reactor at 100 °C for 15 min. The reaction mixture was cooled, and the resulting precipitate was collected by filtration, rinsed with water, and dried under vacuum to yield 105.6 mg (62%) of *N*-(1-(3-chlorophenyl)-3-methyl-1*H*-pyrazol-5-yl)-5-(methylamino)-pyrazolo[1,5-*a*]pyrimidine-3-carboxamide. ^{1}H NMR (400 MHz, DMSO-d_6) δ: 9.93 (s, 1H), 8.55 (d, J = 7.6 Hz, 1H), 8.22 (s, 1H), 8.02 (d, J = 4.3 Hz, 1H), 7.64 (t, J = 1.8 Hz, 1H), 7.57−7.52 (m, 1H), 7.50 (t, J = 7.8 Hz, 1H), 7.47−7.42 (m, 1H), 6.46 (s, 1H), 6.33 (d, J = 7.6 Hz, 1H), 2.25−2.19 (m, 6H). MS: m/z 382.1 ([M + H]$^+$).

*5-Amino-N-(3-(3-chlorophenyl)-1-methyl-1H-pyrazol-4-yl)-pyrazolo[1,5-a]pyrimidine-3-carboxamide (**7c**).* Ammonia gas was bubbled through a stirring 0 °C suspension of **6b** (60 mg, 0.2 mmol) and ethanol (3 mL) for 20 min. The reaction vessel was capped and subjected to microwave irradiation at 120 °C for 90 min. After the reaction mixture was cooled to ambient temperature, the resulting precipitate was collected by filtration, rinsed with ethanol, and dried under vacuum to yield 47.5 mg (80%) of 5-amino-*N*-(3-(3-chlorophenyl)-1-methyl-1*H*-pyrazol-4-yl)pyrazolo[1,5-*a*]pyrimidine-3-carboxamide. ^{1}H NMR (400 MHz, DMSO-d_6) δ: 9.57 (s, 1H), 8.66 (d, J = 7.6 Hz, 1H), 8.20 (s, 1H), 8.07 (s, 1H), 7.78−7.69 (m, 2H), 7.46 (t, J = 7.8 Hz, 1H), 7.39 (d, J = 8.0 Hz, 1H), 6.40 (d, J = 7.6 Hz, 1H), 3.90 (s, 3H). MS: m/z 368.1 ([M + H]$^+$).

*N-(1-(3-Chlorophenyl)-3-methyl-1H-pyrazol-5-yl)pyrazolo[1,5-a]-pyrimidine-3-carboxamide (**8**).* To pyrazolo[1,5-*a*]pyrimidine-3-carboxylic acid (202 mg, 1.24 mmol) was added phosphoryl chloride (5.35 mL, 57.4 mmol) and then dropwise DIPEA (0.647 mL, 3.72 mmol). The reaction mixture was heated at reflux (130 °C) for 2.5 h. The solvents were then removed under reduced pressure, exchanging the solvent with DCM 4 times. The resulting residue was dissolved in DCM (20 mL), and 1-(3-chlorophenyl)-3-methyl-1*H*-pyrazol-5-amine (385.7 mg, 1.857 mmol) and DIPEA (0.431 mL, 2.48 mmol) were added. The reaction mixture was stirred at ambient temperature for 5 h and then partitioned between ethyl acetate and water. The organic portion was washed with water and brine, dried over magnesium sulfate, and concentrated. The crude product was purified by preparative reverse-phase HPLC and lyophilized to yield 151 mg (35%) of *N*-(1-(3-chlorophenyl)-3-methyl-1*H*-pyrazol-5-yl)pyrazolo-[1,5-*a*]pyrimidine-3-carboxamide. ^{1}H NMR (400 MHz, DMSO-d_6) δ: 10.32 (s, 1H), 9.36 (dd, J = 7.0, 1.6 Hz, 1H), 8.71 (s, 1H), 8.66 (dd, J = 4.2, 1.6 Hz, 1H), 7.77−7.76 (m, 1H), 7.66−7.59 (m, 2H), 7.56−7.51 (m, 1H), 7.31 (dd, J = 7.0, 4.3 Hz, 1H), 6.58 (s, 1H), 2.25 (s, 3H). MS: m/z 353.1 ([M + H]$^+$).

*N-(2-Bromopyridin-3-yl)pyrazolo[1,5-a]pyrimidine-3-carboxamide (**9a**).* To a suspension of pyrazolo[1,5-*a*]pyrimidine-3-carboxylic acid (253.9 mg, 1.556 mmol) in DCM (10 mL) was added DMF (0.1 mL) followed by oxalyl chloride (2.0 M in DCM, 1.0 mL, 2.0 mmol). The reaction mixture was stirred at ambient temperature for 30 min, and then additional oxalyl chloride (0.8 mL, 1.6 mmol) was added. After a further 30 min, the reaction mixture was concentrated. The resulting residue was resuspended in DCM (10 mL), and 2-bromopyridin-3-amine (215.4 mg, 1.245 mmol) and triethylamine (0.8 mL, 6 mmol) were added. The reaction mixture was stirred at ambient temperature for 1.5 h and then concentrated onto silica gel. The crude product was purified via flash chromatography on silica gel (gradient elution: 20−80% ethyl acetate in DCM) to yield 151.3 mg (38%) of *N*-(2-bromopyridin-3-yl)pyrazolo[1,5-*a*]pyrimidine-3-carboxamide. MS: m/z 317.9 ([M + H]$^+$).

*N-(2-(3-Chlorophenyl)pyridin-3-yl)pyrazolo[1,5-a]pyrimidine-3-carboxamide (**10a**).* A mixture of **9a** (76.2 mg, 0.240 mmol), 3-chlorobenzeneboronic acid (100.2 mg, 0.6408 mmol), bis-(triphenylphosphine)palladium(II) chloride (22.6 mg, 0.032 mmol), sodium carbonate (1.0 M aqueous solution, 1.0 mL, 1.0 mmol), and acetonitrile (3.0 mL) was subjected to microwave irradiation at 120 °C for 30 min. The reaction mixture was partitioned between ethyl acetate and water, and the organic layer was dried over magnesium sulfate, filtered, and concentrated. The crude product was purified by reverse phase HPLC and lyophilized to give 49.4 mg (59%) of *N*-(2-(3-chlorophenyl)pyridin-3-yl)pyrazolo[1,5-*a*]pyrimidine-3-carboxamide. ^{1}H NMR (400 MHz, DMSO-d_6) δ: 9.97 (s, 1H), 9.33 (dd, J = 7.0, 1.6 Hz, 1H), 8.82 (dd, J = 8.3, 1.4 Hz, 1H), 8.69 (s, 1H), 8.42 (dd, J = 4.6, 1.4 Hz, 1H), 8.39 (dd, J = 4.2, 1.6 Hz, 1H), 7.71−7.69 (m, 1H), 7.63−7.58 (m, 3H), 7.49 (dd, J = 8.4, 4.6 Hz, 1H), 7.27 (dd, J = 7.0, 4.2 Hz, 1H). MS: m/z 350.0 ([M + H]$^+$).

*N-(4-Bromo-1-methyl-1H-pyrazol-3-yl)pyrazolo[1,5-a]-pyrimidine-3-carboxamide (**11**).* A mixture of pyrazolo[1,5-*a*]-pyrimidine-3-carboxylic acid (165.5 mg, 1.014 mmol), 4-bromo-1-methyl-1*H*-pyrazol-3-amine (177.4 mg, 1.008 mmol), HATU (497.0 mg, 1.307 mmol), DIPEA (0.25 mL, 1.4 mmol), 4-dimethylaminopyridine (33.8 mg, 0.277 mmol), and 5 mL of DMF was heated at 50 °C for 4 days. The reaction mixture was partitioned between ethyl acetate and water, and the organic portion washed with brine, dried over magnesium sulfate, filtered, and concentrated. The crude product was purified by flash chromatography on silica gel (gradient elution: 20−80% ethyl acetate in 5% methanol:DCM) to yield 203.6 mg (63%) of *N*-(4-bromo-1-methyl-1*H*-pyrazol-3-yl)pyrazolo[1,5-*a*]pyrimidine-3-carboxamide. ^{1}H NMR (400 MHz, CD_3OD) δ: 9.17 (dd, J = 7.0, 1.6

Hz, 1H), 8.85 (dd, J = 4.2, 1.6 Hz, 1H), 8.68 (s, 1H), 7.76 (s, 1H), 7.28 (dd, J = 7.0, 4.2 Hz, 1H), 3.88 (s, 3H). MS: m/z 321.1 ([M + H]$^+$).

*N-(1-Methyl-4-(3-chlorophenyl)-1H-pyrazol-3-yl)pyrazolo[1,5-a]-pyrimidine-3-carboxamide (**12**).* To a mixture of **11** (59.5 mg, 0.185 mmol) and 3-chlorobenzeneboronic acid (44.6 mg, 0.285 mmol) in diglyme (5.0 mL) was added sodium carbonate (2 M aqueous solution, 0.3 mL, 0.6 mmol) and tetrakis(triphenylphosphine)-palladium(0) (19.5 mg, 0.0169 mmol). The reaction mixture was purged with nitrogen and then stirred at 100 °C for 24 h. The reaction mixture was partitioned between ethyl acetate and water and the organic portion washed with brine, dried over magnesium sulfate, filtered, and concentrated. The crude product was purified by reverse phase HPLC and lyophilized to yield 4.3 mg (7%) of *N*-(1-methyl-4-(3-chlorophenyl)-1*H*-pyrazol-3-yl)pyrazolo[1,5-*a*]pyrimidine-3-carboxamide. ^{1}H NMR (400 MHz, DMSO-d_6) δ: 9.70 (s, 1H), 9.38 (dd, J = 7.0, 1.6 Hz, 1H), 8.86 (dd, J = 4.2, 1.6 Hz, 1H), 8.68 (s, 1H), 8.16 (s, 1H), 7.56 (t, J = 1.8 Hz, 1H), 7.45 (d, J = 7.9 Hz, 1H), 7.35–7.34 (m, 1H), 7.32 (d, J = 7.7 Hz, 1H), 7.23 (d, J = 8.0 Hz, 1H), 3.86 (s, 3H). MS: m/z 353.0 ([M + H]$^+$).

*N-(3-(3-Chlorophenyl)-1-methyl-1H-pyrazol-4-yl)pyrazolo[1,5-a]-pyrimidine-3-carboxamide (**13a**).* A mixture of **20a** (400.0 mg, 1.926 mmol), pyrazolo[1,5-*a*]pyrimidine-3-carboxylic acid (342.9 mg, 2.102 mmol), 7-azabenzotriazol-1-yloxy-tris-(pyrrolidino)phosphonium hexafluorophosphate (PyAOP) (1.205 g, 2.324 mmol), DIPEA (0.80 mL, 4.6 mmol), and 4-dimethylaminopyridine (43.4 mg, 0.355 mmol) in 15.0 mL DMF was stirred at 50 °C for 15 h. The reaction mixture was partitioned between DCM and water and the aqueous layer extracted once more with DCM. The combined organic portions were dried over magnesium sulfate and concentrated onto silica gel. The crude product was separated by flash chromatography on silica gel (solvent gradient: 0–70% ethyl acetate (containing 2% methanol) in DCM). The resulting solid material was triturated with ethyl acetate, sonicated, and the solids were collected by filtration and dried under vacuum to yield 0.502 g (74%) of *N*-(3-(3-chlorophenyl)-1-methyl-1*H*-pyrazol-4-yl)pyrazolo[1,5-a]pyrimidine-3-carboxamide. ^{1}H NMR (400 MHz, DMSO-d_6) δ: 10.00 (s, 1H), 9.38 (dd, J = 7.0, 1.6 Hz, 1H), 8.84 (dd, J = 4.2, 1.6 Hz, 1H), 8.70 (s, 1H), 8.33 (s, 1H), 7.84 (t, J = 1.8 Hz, 1H), 7.77 (dt, J = 7.8, 1.8 Hz, 1H), 7.57 (t, J = 7.9 Hz, 1H), 7.47 (d, J = 7.9 Hz, 1H), 7.34 (dd, J = 7.0, 4.2 Hz, 1H), 3.93 (s, 3H). MS: m/z 353.0 ([M + H]$^+$).

*N-(3-(3-Chlorophenyl)-1-isopropyl-1H-pyrazol-4-yl)pyrazolo[1,5-a]pyrimidine-3-carboxamide (**14a**).* **13b** (68.9 mg, 0.203 mmol) was dissolved in 4 mL of DMF. To this solution was added cesium carbonate (148 mg, 0.454 mmol) and isopropyl iodide (23.0 μL, 0.230 mmol). The reaction mixture was stirred at 50 °C for 2 h. The reaction mixture was then partitioned between ethyl acetate and water and the organic portion washed with brine, dried over magnesium sulfate, and concentrated. The crude product was purified by reverse phase HPLC and lyophilized to give 47.2 mg (61%) of *N*-(3-(3-chlorophenyl)-1-isopropyl-1*H*-pyrazol-4-yl)pyrazolo[1,5-*a*]pyrimidine-3-carboxamide. ^{1}H NMR (400 MHz, DMSO-d_6) δ: 9.99 (s, 1H), 9.38 (dd, J = 7.0, 1.6 Hz, 1H), 8.84 (dd, J = 4.2, 1.6 Hz, 1H), 8.70 (s, 1H), 8.36 (s, 1H), 7.85 (t, J = 1.8 Hz, 1H), 7.78 (td, J = 7.7, 1.4 Hz, 1H), 7.57 (t, J = 7.9 Hz, 1H), 7.50–7.44 (m, 1H), 7.34 (dd, J = 7.0, 4.2 Hz, 1H), 4.66–4.51 (m, 1H), 1.49 (d, J = 6.7 Hz, 6H). MS: m/z 381.1 ([M + H]$^+$).

*N-(3-(3-Chlorophenyl)-1-(2-hydroxy-2-methylpropyl)-1H-pyrazol-4-yl)pyrazolo[1,5-a]pyrimidine-3-carboxamide (**14f**).* **13b** (58.9 mg, 0.174 mmol) was dissolved in 5 mL of DMF. To this solution was added isobutylene oxide (0.5 mL, 6 mmol) and cesium carbonate (56.4 mg, 0.173 mmol). The reaction mixture was stirred at 50 °C for 7.5 h. The reaction mixture was then partitioned between ethyl acetate and water and the organic portion washed with brine, dried over magnesium sulfate, and concentrated. The crude product was purified by reverse phase HPLC and lyophilized to give 33.1 mg (46%) of *N*-(3-(3-chlorophenyl)-1-(2-hydroxy-2-methylpropyl)-1*H*-pyrazol-4-yl)-pyrazolo[1,5-*a*]pyrimidine-3-carboxamide. ^{1}H NMR (400 MHz, DMSO-d_6) δ: 10.02 (s, 1H), 9.37 (dd, J = 7.0, 1.5 Hz, 1H), 8.84 (dd, J = 4.2, 1.6 Hz, 1H), 8.69 (s, 1H), 8.35 (s, 1H), 7.84 (t, J = 1.7 Hz, 1H), 7.77 (d, J = 7.8 Hz, 1H), 7.58 (t, J = 7.9 Hz, 1H), 7.48 (dd, J = 8.0, 1.0 Hz, 1H), 7.33 (dd, J = 7.0, 4.2 Hz, 1H), 4.73 (s, 1H), 4.09 (s, 2H), 1.13 (s, 6H). MS: m/z 411.1 ([M + H]$^+$).

*5-Bromo-2-methylpyridine 1-oxide (**15**).* A solution of 5-bromo-2-methylpyridine (2.0 g, 12 mmol) and *m*-chloroperoxybenzoic acid (70%, 2.89 g, 12.9 mmol) in 30 mL of chloroform was stirred at room temperature for 4 h. The reaction mixture was then partitioned between DCM and 2 M aqueous sodium carbonate. The aqueous layer was extracted once more with DCM, and the combined organic portions were dried over magnesium sulfate, filtered, and concentrated to yield 2.1575 g (99%) of 5-bromo-2-methylpyridine 1-oxide. ^{1}H NMR (400 MHz, DMSO-d_6) δ: 8.57 (d, J = 1.4 Hz, 1H), 7.51 (dd, J = 8.4, 1.6 Hz, 1H), 7.44 (d, J = 8.4 Hz, 1H), 2.30 (s, 3H). MS: m/z 189.0 ([M + H]$^+$).

*5-Bromo-2-methyl-4-nitropyridine 1-oxide (**16**).* **15** (2.269 g, 12.07 mmol) was dissolved in sulfuric acid (4 mL, 80 mmol) and cooled in an ice–water bath. Fuming nitric acid (3 mL, 60 mmol) was added dropwise. After addition of the nitric acid was complete, the reaction mixture was first warmed to room temperature and then heated to 90 °C. After heating for 2 h, the reaction mixture was cooled in an ice–water bath and slowly adjusted to pH 10 with 2 M aqueous sodium carbonate. This mixture was extracted twice with DCM. The combined organic extracts were dried over magnesium sulfate, filtered, and concentrated to yield 2.54 g (90%) of 5-bromo-2-methyl-4-nitropyridine 1-oxide. MS: m/z 233.0 ([M + H]$^+$).

*5-Bromo-2-methylpyridin-4-amine (**17**).* To a solution of **16** (2.54 g, 10.9 mmol) in 10 mL of concentrated hydrochloric acid was added tin chloride dihydrate (9.96 g, 43.75 mmol). The reaction mixture was heated at 90 °C for 24 h, at which time additional tin chloride dihydrate (3.15 g, 13.84 mmol) and 5 mL of concentrated hydrochloric acid were added. The reaction mixture was held at 90 °C for an additional 24 h and then cooled to room temperature and adjusted to neutral pH with 2 M aqueous sodium carbonate. The resulting mixture was extracted three times with DCM, and the combined organic extracts dried over magnesium sulfate, filtered, and concentrated to yield 1.15 g (56%) of 5-bromo-2-methylpyridin-4-amine. ^{1}H NMR (400 MHz, DMSO-d_6) δ: 8.07 (s, 1H), 6.51 (s, 1H), 6.13 (s, 2H), 2.22 (s, 3H). MS: m/z 187.2 ([M + H]$^+$).

*2-(2-(3-Chlorophenyl)-2-oxoethylisoindoline-1,3-dione (**18a**).* A mixture of 2-bromo-3′-chloroacetophenone (0.927 g, 3.97 mmol) and potassium phthalimide (0.813 g, 4.39 mmol) in 15 mL of DMF was stirred at 50 °C for 1 h. The solvent was removed under vacuum, and the resulting solids were triturated with ethyl acetate and filtered. The collected solids were dried under vacuum to give 2-(2-(3-chlorophenyl)-2-oxoethylisoindoline-1,3-dione, which was carried forward without further purification. ^{1}H NMR (400 MHz, DMSO-d_6) δ: 8.13 (t, J = 1.9 Hz, 1H), 8.06 (d, J = 7.9 Hz, 1H), 8.00–7.90 (m, 4H), 7.85–7.80 (m, 1H), 7.65 (t, J = 7.9 Hz, 1H), 5.29 (s, 2H).

*Di-tert-butyl 2-(2,5-Dimethylphenyl)-2-oxoethyliminodicarbonate (**18b**).* In an oven-dried flask, di-*tert*-butyl iminodicarboxylate (2.566 g, 11.81 mmol) was combined with sodium hydride (60 wt % in mineral oil, 0.59 g, 15 mmol) and 30 mL of DMF. The reaction mixture was stirred at ambient temperature for 1.5 h, and then 2-bromo-1-(2,5-dimethylphenyl)ethanone (2.432 g, 10.71 mmol) was added. The reaction was stirred at ambient temperature for an additional 1.5 h and then partitioned between ethyl acetate and water. The organic portion was washed with water and brine, dried over magnesium sulfate, and concentrated under vacuum. The crude product was purified by flash chromatography on silica gel (gradient elution: 0–40% ethyl acetate in heptanes) to obtain 3.008 g (77%) of di-*tert*-butyl 2-(2,5-dimethylphenyl)-2-oxoethyl-iminodicarbonate. MS: m/z 386.2 ([M + Na]$^+$).

*2-(3-(3-Chlorophenyl)-1-(dimethylamino)-3-oxoprop-1-en-2-yl)-isoindoline-1,3-dione (**19a**).* A stirred mixture of **18a** (782.2 mg, 2.610 mmol) and DMFDMA (1.5 mL, 11 mmol) was heated at 100 °C for 18 h. Excess DMFDMA was removed under vacuum. The crude product was purified by flash chromatography on silica gel (gradient elution: 50–100% ethyl acetate in heptanes) to yield 740 mg (80%) of 2-(3-(3-chlorophenyl)-1-(dimethylamino)-3-oxoprop-1-en-2-yl)-isoindoline-1,3-dione. ^{1}H NMR (400 MHz, $CDCl_3$) δ: 7.91 (dd, J = 5.4, 3.1 Hz, 2H), 7.76 (dd, J = 5.5, 3.1 Hz, 2H), 7.57 (s, 1H), 7.45 (d, J

= 7.5 Hz, 1H), 7.42−7.35 (m, 2H), 7.31 (t, J = 7.8 Hz, 1H), 3.00 (s, 6H). MS: m/z 355.2 ([M + H]$^+$).

*3-(3-Chlorophenyl)-1-methyl-1H-pyrazol-4-amine (**20a**).* To a solution of **19a** (2.30 g, 6.48 mmol) in 50 mL of ethanol was added *N*-methylhydrazine (1.4 mL, 26 mmol). The reaction mixture was stirred at 80 °C for 2 h and then concentrated onto silica gel. The crude mixture of regioisomers was separated and purified by flash chromatography on silica gel (gradient elution: 0−80% ethyl acetate in DCM) to yield 715.0 mg (53%) of 3-(3-chlorophenyl)-1-methyl-1*H*-pyrazol-4-amine. ^{1}H NMR (400 MHz, $CDCl_3$) δ: 7.78 (t, J = 1.8 Hz, 1H), 7.64 (dt, J = 7.7, 1.4 Hz, 1H), 7.33 (t, J = 7.8 Hz, 1H), 7.28−7.23 (m, 2H), 7.04 (s, 1H), 3.84 (s, 3H). MS: m/z 208.2 ([M + H]$^+$). Also isolated was 274.6 mg (20%) of 5-(3-chlorophenyl)-1-methyl-1*H*-pyrazol-4-amine. ^{1}H NMR (400 MHz, $CDCl_3$) δ: 7.46−7.40 (m, 1H), 7.40−7.35 (m, 2H), 7.29−7.25 (m, 1H), 7.23 (s, 1H), 3.76 (s, 3H). MS: m/z 208.2 ([M + H]$^+$).

*Ethyl 3-(5-Chloro-2-methylphenyl)-3-oxopropanoate (**21a**).* To a stirring solution of 5-chloro-2-methylbenzoic acid (4.8547 g, 28.458 mmol) in 30 mL of THF was added *N*,*N*-carbonyldiimidazole (4.8688 g, 30.027 mmol). Stirring was continued at ambient for 30 min to generate the acyl-imidazole. Separately, potassium ethyl malonate (11.612 g, 68.224 mmol) and $MgCl_2$ (3.2689 g, 34.333 mmol) were suspended in 50 mL of THF. To the magnesium chloride mixture was added the acyl-imidazole solution. The resulting reaction mixture was heated at 50 °C for 10 h. The reaction mixture was partitioned between ethyl acetate and water, and the organic portion dried over magnesium sulfate, filtered through a pad of Celite, and concentrated to provide 8.07 g of ethyl 3-(5-chloro-2-methoxyphenyl)-3-oxopropanoate, which was used without purification. MS: m/z 241.2 ([M + H]$^+$).

*Ethyl 3-(2,6-Dichlorophenyl)-3-oxopropanoate (**21b**).* Potassium ethyl malonate (63.0 g, 370 mmol) was placed in a flask under nitrogen. Acetonitrile (1 L) was added, and the mixture was cooled to 10−15 °C. To the cooled solution was added triethylamine (55 mL, 0.39 mol) followed by $MgCl_2$ (42.8 g, 0.449 mol), and the mixture was then stirred at ambient temperature for 2.5 h. After cooling the reaction mixture to 0 °C, 2,6-dichlorobenzoyl chloride (37.7 g, 180 mmol) was added slowly over 25 min, followed by addition of more triethylamine (5 mL, 40 mmol). The reaction mixture was stirred at ambient temperature overnight. The solvent was removed under reduced pressure and the residue partitioned between toluene and 10% aqueous HCl. The organic layer was concentrated to provide a quantitative yield of ethyl 3-(2,6-dichlorophenyl)-3-oxopropanoate, which was carried forward without purification.

*Ethyl 2-(5-Chloro-2-methylbenzoyl)-3-(dimethylamino)acrylate (**22a**).* A stirred mixture of **21a** (28.458 mmol) and DMFDMA (10.0 mL, 75.3 mmol) was heated at 90 °C for 3 h. After evaporation of excess DMFDMA under reduced pressure, the crude product was purified by flash chromatography on silica gel (gradient elution: 0−80% ethyl acetate in DCM) to yield 2.87 g (34%) of ethyl 2-(5-chloro-2-methylbenzoyl)-3-(dimethylamino)acrylate. MS: m/z 296.3 ([M + H]$^+$).

*Ethyl 5-(5-Chloro-2-methylphenyl)-1H-pyrazole-4-carboxylate (**23**).* A solution of **22a** (2.87 g, 9.70 mmol) and hydrazine (0.50 mL, 16.0 mmol) in 30 mL of ethanol was heated at 70 °C for 2 h. The crude reaction mixture was concentrated under vacuum to provide 2.57 g (100%) ethyl 5-(5-chloro-2-methoxyphenyl)-1*H*-pyrazole-4-carboxylate, which was used without further purification. MS: m/z 265.2 ([M + H]$^+$).

*Ethyl 3-(5-Chloro-2-methylphenyl)-1-methyl-1H-pyrazole-4-carboxylate (**24a**) and Ethyl 5-(5-Chloro-2-methylphenyl)-1-methyl-1H-pyrazole-4-carboxylate (**25**).* To a solution of **23** (9.70 mmol) in 35 mL of DMF was added cesium carbonate (3.831 g, 11.76 mmol) and iodomethane (0.90 mL, 14 mmol). The reaction mixture was stirred at 40 °C for 7 h and was then partitioned between ethyl acetate and water. The organic portion was dried over magnesium sulfate and concentrated. The crude product was purified by flash chromatography on silica gel (gradient elution: 0−40% ethyl acetate in DCM) to yield 2.179 g (81%) of a 1:1 mixture of the regioisomeric products, ethyl 3-(5-chloro-2-methylphenyl)-1-methyl-1*H*-pyrazole-4-carboxylate, and ethyl 5-(5-chloro-2-methylphenyl)-1-methyl-1*H*-pyrazole-4-carboxylate. MS: m/z 279.2 ([M + H]$^+$).

*Ethyl 3-(2,6-Dichlorophenyl)-1-methyl-1H-pyrazole-4-carboxylate (**24b**).* To a stirred solution of **22b** (12.6 g, 40 mmol) in acetic acid (100 mL) was added *N*-methyl-hydrazine (3.84 g, 83.4 mmol). The reaction mixture was stirred at ambient temperature for 3 days. The mixture was then concentrated under reduced pressure, and the residue was partitioned between ethyl acetate and water. The organic portion was dried over magnesium sulfate and concentrated under vacuum. The crude product was purified by flash chromatography on silica gel to yield 5.4 g (45%) of ethyl 3-(2,6-dichlorophenyl)-1-methyl-1*H*-pyrazole-4-carboxylate. MS: m/z 298.9 ([M + H]$^+$).

*3-(5-Chloro-2-methylphenyl)-1-methyl-1H-pyrazol-4-amine (**26a**) and 5-(5-Chloro-2-methylphenyl)-1-methyl-1H-pyrazol-4-amine (**27**).* To a solution of **24a** and **25** (1:1 mixture of regioisomers, 2.179 g, 7.818 mmol) in ethanol (10 mL) was added 1 M aqueous NaOH (18 mL, 18 mmol). The reaction mixture was heated at 50 °C for 20 h, and then the solvent was removed under reduced pressure. The resulting residue was adjusted to pH 2 with 1 M aqueous H_3PO_4 and extracted with DCM (3 × 100 mL). The combined organic extracts were dried over magnesium sulfate, filtered, and concentrated under vacuum. The resulting material was dissolved in 1,4-dioxane (15 mL) and treated with triethylamine (2.20 mL, 15.8 mmol) and diphenylphosphonic azide (1.90 mL, 8.82 mmol). The mixture was stirred at ambient temperature for 1 h and then treated with *tert*-butyl alcohol (15 mL) and heated at 90 °C for 1 h. After being cooled to room temperature, the mixture was partitioned between ethyl acetate and water. The organic portion was dried over magnesium sulfate and concentrated. The crude product was purified by flash chromatography on silica gel (solvent gradient: 0−50% ethyl acetate in DCM) to yield a mixture of the title compounds as the *tert*-butyl-carbamates (1.637 g, 66%). To a solution of this material (1:1 mixture of regioisomers, 1.637 g, 5.088 mmol) in 10 mL of DCM was added hydrogen chloride (10.0 mL of a 4.0 M solution in 1,4-dioxane, 40 mmol). The reaction mixture was stirred at ambient temperature for 16 h and then evaporated to dryness. The solid residue was partitioned between DCM and a saturated aqueous solution of sodium bicarbonate. The aqueous portion was extracted once more with DCM, and the combined organic extracts were dried over magnesium sulfate, filtered, and concentrated under vacuum. The crude product was purified and regioisomers separated by flash chromatography on silica gel (gradient elution: 0−100% ethyl acetate in DCM) to yield 429.7 mg (38%) of 3-(5-chloro-2-methylphenyl)-1-methyl-1*H*-pyrazol-4-amine (**26a**). ^{1}H NMR (400 MHz, $CDCl_3$) δ: 7.35 (d, J = 1.8 Hz, 1H), 7.24−7.17 (m, 2H), 7.04 (s, 1H), 3.84 (s, 3H), 2.76 (s, 2H), 2.30 (s, 3H). MS, m/z 222.1 ([M + H]$^+$). And 420.2 mg (37%) of 5-(5-chloro-2-methylphenyl)-1-methyl-1*H*-pyrazol-4-amine (**27**). ^{1}H NMR (400 MHz, $CDCl_3$) δ: 7.33 (dd, J = 8.3, 2.1 Hz, 1H), 7.28 (s, 1H), 7.24−7.19 (m, 2H), 3.57 (s, 3H), 2.71 (s, 2H), 2.15 (s, 3H). MS: m/z 222.1 ([M + H]$^+$).

*4-Nitro-1-((2-(trimethylsilyl)ethoxy)methyl)-1H-pyrazole (**28**).* In an oven-dried flask equipped with a stir bar, 4-nitro-1*H*-pyrazole (6.598 g, 58.35 mmol) was dissolved in 50 mL of THF. Sodium hydride (60 wt % dispersion in mineral oil, 4.827 g, 120.7 mmol) was added while cooling the reaction vessel with an ice−water bath, and the reaction was then stirred at ambient temperature for 10 min. [β-(Trimethylsilyl)ethoxy]methyl chloride (12.0 mL, 67.8 mmol) was then added, and the reaction stirred at ambient temperature for 1.5 h. The reaction mixture was quenched with 50 mL of water and extracted into ethyl acetate. The organic extract was dried over magnesium sulfate, filtered, and concentrated under vacuum. The resulting crude product was purified by flash chromatography on silica gel (gradient elution: 0−30% ethyl acetate in heptanes) to obtain 14.1368 g (99%) of 4-nitro-1-((2-(trimethylsilyl)ethoxy)methyl)-1*H*-pyrazole. ^{1}H NMR (400 MHz, $CDCl_3$) δ: 8.30 (s, 1H), 8.10 (s, 1H), 5.45 (s, 2H), 3.73−3.54 (m, 2H), 1.02−0.84 (m, 2H), −0.00 (s, 9H). MS: m/z 244.2 ([M + H]$^+$).

*5-(5-Chloro-2-methoxyphenyl)-4-nitro-1-((2-(trimethylsilyl)-ethoxy)methyl)-1H-pyrazole (**29**).* To a solution of **28** (4.259 g, 17.50 mmol) in 40 mL DMF was added 2-bromo-4-chloroanisole (3.35 mL,

24.6 mmol), palladium(II) acetate (197.2 mg, 0.8784 mmol), di(1-adamantyl)-*n*-butylphosphine (469.5 mg, 1.309 mmol), potassium carbonate (7.2763 g, 52.648 mmol), and trimethylacetic acid (0.4523 g, 4.428 mmol). While stirring at room temperature, nitrogen gas was bubbled through the reaction mixture for 10 min, and the reaction was then heated under a nitrogen balloon at 120 °C for 6 h. The reaction mixture was then cooled to room temperature, diluted into ethyl acetate, washed with water and brine, dried over magnesium sulfate, filtered, and concentrated under vacuum. The crude product was purified by flash chromatography on silica gel (gradient elution: 0−25% ethyl acetate in heptanes) to obtain 6.719 g (89%) of 3-(5-chloro-2-methoxyphenyl)-4-nitro-1-((2-(trimethylsilyl)ethoxy)methyl)-1*H*-pyrazole. ^{1}H NMR (400 MHz, $CDCl_3$) δ 8.22 (s, 1H), 7.47 (dd, J = 8.9, 2.6 Hz, 1H), 7.36 (d, J = 2.5 Hz, 1H), 6.96 (d, J = 8.9 Hz, 1H), 5.34−5.20 (m, 2H), 3.76 (s, 3H), 3.69−3.46 (m, 2H), 0.96−0.79 (m, 2H), −0.02 (s, 9H). MS: m/z 384.2 ($[M + H]^+$).

*5-(5-Chloro-2-methoxyphenyl)-1-((2-(trimethylsilyl)ethoxy)-methyl)-1H-pyrazol-4-amine (**30**).* To a solution of **29** (5.97 g, 15.6 mmol) in 25 mL of ethanol was added water (50 mL), ammonium chloride (3.367 g, 62.94 mmol), and iron powder (4.367 g, 78.2 mmol). The reaction mixture was heated at 75 °C for 1.5 h. After being cooled to ambient temperature, the mixture was diluted with DCM and filtered through a Celite pad, rinsing with more DCM. The combined filtrate was added to 150 mL of saturated aqueous sodium bicarbonate and extracted twice with DCM. The combined organic extracts were dried over magnesium sulfate, filtered, and concentrated under vacuum to yield 5.50 g (100%) of 3-(5-chloro-2-methoxyphenyl)-1-((2-(trimethylsilyl)ethoxy)methyl)-1*H*-pyrazol-4-amine, which was carried forward without purification. ^{1}H NMR (500 MHz, $CDCl_3$) δ 7.44 (d, J = 2.6 Hz, 1H), 7.35 (dd, J = 8.8, 2.6 Hz, 1H), 7.28 (s, 1H), 6.93 (d, J = 8.9 Hz, 1H), 5.24 (s, 2H), 3.82 (s, 3H), 3.52 (t, J = 8.2 Hz, 2H), 0.91−0.79 (m, 2H), −0.04 (s, 9H). MS: m/z 354.3 ($[M + H]^+$).

*3-(3-Chlorophenyl)-3-oxopropoinic Acid Ethyl Ester (**31**).* Sodium hydride (60% in mineral oil, 1.03 g, 25.9 mmol) was added to a stirred solution of diethyl carbonate (3.9 mL, 32 mmol) in toluene (25 mL), under nitrogen. 3-Chloroacetophenone (0.84 mL, 6.5 mmol) in toluene (5 mL) was then added dropwise to the suspension over 30 min. The resulting mixture was heated to reflux for 16 h. After cooling, the reaction was carefully quenched with acetic acid (20 mL). Water (20 mL) was added and the mixture extracted into ethyl acetate (3×). The combined organic extracts were washed with saturated aqueous sodium bicarbonate solution, dried with anhydrous sodium sulfate, and concentrated under reduced pressure to yield a dark-orange oil, which was purified by Kugelrohr bulb to bulb distillation, at 150 °C, under vacuum, to yield 0.996 g of a colorless oil. Further purification by flash chromatography on silica gel (gradient elution: 0−15% ethyl acetate in cyclohexane) afforded 0.75 g (51%) of 3-(3-chlorophenyl)-3-oxopropoinic acid ethyl ester, 2:1 mixture of keto−enol tautomers, as a colorless oil. ^{1}H NMR (300 MHz, $CDCl_3$) δ: 12.56 (s, 1H), 7.93 (t, J = 1.9 Hz, 1H), 7.83 (ddd, J = 7.8, 1.7, 1.1 Hz, 1H), 7.77 (t, J = 1.9 Hz, 1H), 7.65 (dt, J = 7.7, 1.5 Hz, 1H), 7.58 (ddd, J = 8.0, 2.1, 1.1 Hz, 1H), 7.47−7.32 (m, 3H), 5.66 (s, 1H), 4.33−4.16 (m, 4H), 3.98 (s, 2H), 1.35 (t, J = 7.1 Hz, 3H), 1.27 (t, J = 7.1 Hz, 3H).

*5-(3-Chlorophenyl)-isoxazole-4-carboxylic Acid Ethyl Ester (**32**).* DMF-DMA (1.5 mL, 11.6 mmol) was added to a solution of **31** (0.75 g, 3.3 mmol) in DMF (25 mL), under nitrogen. The mixture was heated to reflux for 5 h. After cooling, ethyl acetate and water were added and the layers separated. The organic extract was dried with anhydrous sodium sulfate and concentrated under reduced pressure to yield 0.79 g of a thick orange oil. The residue (0.595 g, ca. 2.11 mmol) was dissolved in methanol (5 mL) and treated with hydroxylamine hydrochloride (0.147 g, 2.11 mmol) at reflux for 1 h. After cooling, ethyl acetate and water were added and the layers separated. The aqueous phase was then extracted with ethyl acetate (2×). The combined organic extracts were dried with anhydrous sodium sulfate and concentrated under reduced pressure to yield an orange solid. Purification by flash chromatography on silica gel (gradient elution: 0−10% ethyl acetate in cyclohexane) afforded 422 mg (79%) of 5-(3-chlorophenyl)-isoxazole-4-carboxylic acid ethyl ester as a white solid. ^{1}H NMR (400 MHz, $CDCl_3$) δ: 8.65 (s, 1H), 8.18 (t, J = 1.9 Hz, 1H), 8.04 (dt, J = 7.7, 1.4 Hz, 1H), 7.53 (ddd, J = 8.1, 2.1, 1.2 Hz, 1H), 7.49−7.44 (m, 1H), 4.37 (q, J = 7.1 Hz, 2H), 1.39 (t, J = 7.1 Hz, 3H).

*5-(3-Chlorophenyl)-isoxazole-4-carboxylic Acid (**33**).* A suspension of **32** (422 mg, 1.68 mmol) in 6 M aqueous HCl (10 mL) and acetic acid (6 mL) was heated to reflux for 5 h. After cooling, ethyl acetate was added to the suspension and the layers were separated. The aqueous layer was then extracted with ethyl acetate (2×). The organic extracts were combined, dried with anhydrous sodium sulfate, and concentrated under reduced pressure to yield 5-(3-chlorophenyl)-isoxazole-4-carboxylic acid as a white solid. This was used in the next step without further purification. ^{1}H NMR (400 MHz, $CDCl_3$) δ: 8.70 (d, J = 2.3 Hz, 1H), 8.13 (d, J = 2.3 Hz, 1H), 8.02 (d, J = 7.9 Hz, 1H), 7.54 (m, 1H), 7.47 (td, J = 7.9, 2.3 Hz, 1H).

*[5-(3-Chlorophenyl)-isoxazole-4-yl]-carbamic Acid tert-Butyl Ester (**34**).* A solution of crude **33** (254 mg, 1.14 mmol) in thionyl chloride (3 mL) was heated to reflux for 3 h. After cooling, the mixture was concentrated under reduced pressure to yield an orange residue. The residue was dissolved in acetone (2 mL) and cooled to 0 °C (ice−water bath). Sodium azide (133 mg, 2.04 mmol) was added, and the resulting mixture was stirred for 1 h and then at ambient temperature for 1 h. Ethyl acetate was added and the layers separated. The organic extract was washed with water (2×) and brine (2×), dried with anhydrous sodium sulfate, and concentrated under reduced pressure to leave an orange solid. The residue was then treated with *tert*-butanol (8 mL) at reflux for 16 h. After cooling, the solvent was removed under vacuum and the residue purified by flash chromatography on silica gel (gradient elution: 0−20% ethyl acetate in cyclohexane) to afford 184 mg (55%) of [5-(3-chlorophenyl)-isoxazole-4-yl]-carbamic acid *tert*-butyl ester as an orange solid. ^{1}H NMR (400 MHz, $CDCl_3$) δ: 7.70 (s, 1H), 7.59 (d, J = 6.9 Hz, 1H), 7.48−7.37 (m, 3H), 1.52 (s, 9H).

*5-(3-Chlorophenyl)-isoxazole-4-ylamine Hydrochloride (**35**).* First, 4 M HCl solution in 1,4-dioxane (1.5 mL, 6.0 mmol) was added to a stirred solution of **34** (184 mg, 0.624 mmol) in 1,4-dioxane (2 mL). Then the resulting mixture was heated to 40 °C for 20 h. After cooling, the mixture was concentrated under reduced pressure to give 147 mg (quant) of 5-(3-chlorophenyl)-isoxazole-4-ylamine hydrochloride as a yellow solid. This was used in the next step without further purification. ^{1}H NMR (400 MHz, CD_3OD) δ: 8.61 (br, m, 1H), 7.85 (br, m, 1H), 7.75 (br, m, 1H), 7.62 (br, m, 2H).

*3-Chlorobenzaldehyde Oxime (**36**).* To a solution of 3-chlorobenzaldehyde (0.81 mL, 7.1 mmol) in EtOH (25 mL) was added hydroxylamine hydrochloride (0.54 g, 7.8 mmol), followed by pyridine (0.57 mL, 7.1 mmol). The resulting colorless mixture was stirred at ambient temperature for 5 h. Then 1 M aqueous HCl was added until pH reached 2, and then the mixture was extracted into DCM (3×). The organic layers were combined and dried with anhydrous sodium sulfate, filtered, and concentrated under reduced pressure to yield 1.22 g (quant) of 3-chlorobenzaldehyde oxime as a white solid. This was used in the next step without further purification. ^{1}H NMR (400 MHz, $CDCl_3$) δ: 8.11 (s, 1H), 7.59 (m, 1H), 7.45 (m, 1H), 7.36 (m, 1H), 7.32 (m, 1H).

*(Z)-3-Chloro-N-hydroxybenzene-1-carbonimidoyl Chloride (**37**).* To a solution of **36** (436 mg, 2.80 mmol) in DMF (8 mL) was added *N*-chlorosuccinimide (307 mg, 2.30 mmol), and the resulting yellow mixture was stirred at ambient temperature for 1.5 h. The reaction was quenched with ice−water and extracted into diethyl ether (2×). The organic layers were combined, washed with water (4×), dried with anhydrous sodium sulfate, filtered, and concentrated under reduced pressure to yield 480 mg (quant) of (*Z*)-3-chloro-*N*-hydroxybenzene-1-carbonimidoyl chloride as an orange solid. This was used in the next step without further purification. ^{1}H NMR (300 MHz, $CDCl_3$) δ: 7.85 (m, 1H), 7.75 (ddd, J = 7.72, 1.75, 1.25 Hz, 1 H), 7.43 (ddd; J = 8.02, 2.06, 1.25 Hz, 1H), 7.36 (m, 1H).

*(E)-3-Pyrrolidin-1-ylacrylic Acid Ethyl Ester (**38**).* To a solution of ethyl propiolate (2.9 mL, 29 mmol) in toluene (20 mL) was added dropwise a solution of pyrrolidine (2.4 mL, 29 mmol) in toluene (5 mL) over 10 min. The resulting orange mixture was stirred at ambient temperature for 16 h and concentrated under reduced pressure to

dx.doi.org/10.1021/jm3012239 | J. Med. Chem. 2012, 55, 10090−10107

leave a thick orange oil, which was purified by Kugelrohr distillation, at 140−150 °C, under vacuum, to afford 4.56 g (94%) of (*E*)-3-pyrrolidin-1-ylacrylic acid ethyl ester as pale-yellow oil. ^{1}H NMR (400 MHz, $CDCl_3$) δ: 7.65 (d, J = 12.9 Hz, 1H), 4.48 (d, J = 12.9 Hz, 1H), 4.13 (q, J = 7.1 Hz, 2H), 3.27 (s, 4H), 1.93 (s, 4H), 1.26 (t, J = 7.1 Hz, 3H).

*3-(3-Chlorophenyl)-isoxazole-4-carboxylic Acid Ethyl Ester (**39**).* A mixture of **38** (0.427 g, 2.52 mmol) and triethylamine (0.413 mL, 2.96 mmol) in diethyl ether (5 mL), under nitrogen, was cooled using an ice bath. To this was added dropwise a solution of **37** (0.48 g, 2.5 mmol) in diethyl ether, over 25 min. A cream-colored solid precipitate formed, and the suspension was stirred at ambient temperature for 18 h. The mixture was partitioned between water and diethyl ether, and the aqueous layer was extracted with diethyl ether. The organic extracts were combined and dried with anhydrous sodium sulfate, filtered, and concentrated under reduced pressure to give a viscous yellow oil. Purification by flash chromatography on silica gel (gradient elution: 0−20% ethyl acetate in cyclohexane) afforded 0.359 g (57%) of 3-(3-chlorophenyl)-isoxazole-4-carboxylic acid ethyl ester as a colorless oil. ^{1}H NMR (400 MHz, $CDCl_3$) δ: 9.02 (s, 1H), 7.81 (ddd, J = 2.1, 1.6, 0.5 Hz, 1H), 7.68 (ddd, J = 7.6, 1.6, 1.2 Hz, 1H), 7.48 (ddd, J = 8.1, 2.1, 1.2 Hz, 1H), 7.43−7.39 (m, 1H), 4.31 (q, J = 7.1 Hz, 2H), 1.32 (t, J = 7.1 Hz, 3H).

*3-(3-Chlorophenyl)-isoxazole-4-carboxylic Acid (**40**).* A stirred solution of **39** (0.359 g, 1.43 mmol) in acetic acid (6 mL) was treated with 6 M aqueous HCl (10 mL) at reflux for 5.5 h. After cooling, ethyl acetate was added causing phase separation of the organic and aqueous layers. The resulting aqueous layer was extracted again with ethyl acetate. The combined organic extracts were dried with anhydrous sodium sulfate, filtered, and concentrated under reduced pressure to yield 0.315 g (99%) of 3-(3-chlorophenyl)-isoxazole-4-carboxylic acid as a white solid. This was used in the next step without further purification. ^{1}H NMR (400 MHz, $CDCl_3$) δ: 9.12 (m, 1H), 7.81 (m, 1H), 7.69 (d, J = 7.6 Hz, 1H), 7.49 (m, 1H), 7.43 (m, 1H).

*[3-(3-Chlorophenyl)-isoxazol-4-yl]-carbamic Acid tert-Butyl Ester (**41**).* A mixture of **40** (0.215 g, 0.962 mmol), diphenylphosphorylazide (0.21 mL, 0.96 mmol), and triethylamine (0.134 mL, 0.961 mmol) in *tert*-butanol was heated to reflux (85 °C) for 16 h. After cooling, ethyl acetate was added and the mixture successively washed with 1 M aqueous HCl (2×), saturated aqueous sodium bicarbonate (2×), and brine (2×). The organic layer was dried with anhydrous sodium sulfate, filtered, and concentrated under reduced pressure to yield a cream-colored residue. Purification by flash chromatography on silica gel (gradient elution: 0−15% ethyl acetate in cyclohexane) afforded 217 mg (77%) of [3-(3-chlorophenyl)-isoxazol-4-yl]-carbamic acid *tert*-butyl ester as a colorless oil. ^{1}H NMR (400 MHz, $CDCl_3$) δ: 8.91 (s, 1H), 7.63 (m, 1H), 7.50 (m, 3H), 6.09 (s, 1H), 1.51 (s, 9H).

*3-(3-Chlorophenyl)-isoxazol-4-ylamine Hydrochloride (**42**).* A solution of **41** (0.217 g, 0.736 mmol) in 1,4-dioxane (2 mL) was treated with 4 M HCl solution in 1,4-dioxane (1.5 mL) at ambient temperature for 20 h. The mixture was concentrated under reduced pressure to yield 165 mg (97%) of 3-(3-chlorophenyl)-isoxazol-4-ylamine hydrochloride as a cream-colored solid. This was used in the next step without further purification. ^{1}H NMR (400 MHz, CD_3OD) δ: 9.06 (s, 1H), 7.80 (td, J = 1.8, 0.5 Hz, 1H), 7.69 (dt, J = 7.2, 1.6 Hz, 1H), 7.63 (m, 1H), 7.59 (m, 1H).

*4-(3-Chlorophenyl)-2-methylthiazol-5-ylamine (**43**).* A mixture of α-amino-(3-chlorophenyl)acetonitrile hydrochloride (0.52 g, 2.6 mmol) and powdered sulfur (80 mg, 2.6 mmol) in ethanol (3 mL) was stirred in a sealed tube at 0 °C. Triethylamine (0.53 mL, 3.8 mmol) and a solution of acetaldehyde in ethanol (0.11 g, 2.6 mmol in 0.5 mL) were added sequentially. The resulting mixture was then heated to 60 °C for 2.5 h. After cooling, mixture was concentrated under reduced pressure, and the resulting residue was then dissolved in ethanol (2 mL) and treated with 1 M aqueous HCl (2 mL) at ambient temperature for 16 h. The pH was then adjusted to 12 (using saturated aqueous sodium carbonate solution) and the mixture extracted into DCM (3 × 10 mL). The combined organic extracts were dried with anhydrous sodium sulfate and concentrated under reduced pressure. The resulting residue was purified using an Isolute SCX-2 cartridge (washing with DCM and eluting with 2 M NH_3 in methanol solution) to afford 0.42 g (73%) of 4-(3-chlorophenyl)-2-methylthiazol-5-ylamine as a pale-orange oil, which solidified on standing. ^{1}H NMR (400 MHz, $CDCl_3$) δ: 7.75 (ddd, J = 2.1, 1.7, 0.4 Hz, 1H), 7.61 (ddd, J = 7.8, 1.7, 1.1 Hz, 1H), 7.33 (m, 1H), 7.23 (ddd, J = 8.0, 2.1, 1.1 Hz, 1H), 3.84 (s, 2 H), 2.58 (s, 3H). MS: m/z 224.9/226.9 ($[M + H]^+$).

Enzyme Assays. The activity of the isolated Jak1, Jak2, Jak3, or Tyk2 kinase domain was measured by monitoring phosphorylation of a peptide derived from Jak3 (Val-Ala-Leu-Val-Asp-Gly-Tyr-Phe-Arg-Leu-Thr-Thr) fluorescently labeled on the N-terminus with 5-carboxyfluorescein using the Caliper LabChip technology (Caliper Life Sciences, Hopkinton, MA). To determine the inhibition constants (K_i), compounds were diluted serially in DMSO and added to 50 μL kinase reactions containing 1.5 nM purified Jak1 enzyme (or 0.2 nM purified Jak2 enzyme or 5 nM purified Jak3 enzyme or 1 nM purified Tyk2 enzyme), 100 mM Hepes pH 7.2, 0.015% Brij-35, 1.5 μM peptide substrate, 25 μM ATP, 10 mM $MgCl_2$, 4 mM DTT at a final DMSO concentration of 2%. Reactions were incubated at 22 °C in 384-well polypropylene microtiter plates for 30 min and then stopped by addition of 25 μL of an EDTA containing solution (100 mM Hepes pH 7.2, 0.015% Brij-35, 150 mM EDTA), resulting in a final EDTA concentration of 50 mM. After termination of the kinase reaction, the proportion of phosphorylated product was determined as a fraction of total peptide substrate using the Caliper LabChip 3000 according to the manufacturer's specifications. K_i values were then determined using the Morrison tight binding model.[42] The activity of ruxolitinib was measured as follows, with data representing either three or four independent experiments and error described as the standard deviation: Jak1 K_i 0.09 nM (±0.01 nM), Jak2 K_i 0.24 nM (±0.04 nM), Jak3 K_i 3.22 nM (±0.27 nM), Tyk2 K_i 0.55 nM (±0.07 nM).

Cell Assays. The activities of compounds in Tables 1, 2, and 4 were determined in cell-based assays that are designed to measure Jak2-dependent signaling. The activity of ruxolitinib was measured in both assay formats as follows, with data representing either two (SET2 format) or five (TF1+EPO format) independent experiments and error described as the standard deviation: pSTAT5 SET2 MSD IC_{50} 1.84 nM (±1.70 nM), pSTAT5 SET2 MSD IC_{50} 6.85 nM (±3.57 nM).

pSTAT5 SET2 MSD Format. Compounds were serially diluted in DMSO and incubated with SET2 cells (German Collection of Microorganisms and Cell Cultures (DSMZ); Braunschweig, Germany), which express the $JAK2^{V617F}$ constitutively active mutant protein, in 96-well microtiter plates for 1 h at 37 °C in RPMI medium at a final cell density of 100000 cells per well and a final DMSO concentration of 0.57%. Compound-mediated effects on STAT5 phosphorylation were then measured in the lysates of incubated cells using the Meso Scale Discovery (MSD) technology (Gaithersburg, Maryland) according to the manufacturer's protocol, and EC_{50} values were determined.

pSTAT5 TF1+EPO MSD Format. Compounds were serially diluted in DMSO and incubated with TF-1 cells (American Type Culture Collection, ATCC), Manassas, VA) in 384-well microtiter plates in OptiMEM medium without phenol red, 1% charcoal/dextran stripped FBS, 0.1 mM NEAA, 1 mM sodium pyruvate (Invitrogen Corp.; Carlsbad, CA) at a final cell density of 100000 cells per well and a final DMSO concentration of 0.2%. Human recombinant EPO (Invitrogen Corp., Carlsbad, CA) was then added at a final concentration of 10 units/mL to the microtiter plates containing the TF-1 cells and compound, and the plates were incubated for 30 min at 37 °C. Compound-mediated effects on STAT5 phosphorylation were then measured in the lysates of cells incubated in the presence of EPO, using the MSD technology (Gaithersburg, Maryland) according to the manufacturer's protocol and IC50 values were determined.

In Vivo Pharmacodynamic Assay. Twenty million SET2 cells containing 1:1 matrigel were inoculated subcutaneously in the right flank of female, 8−12-week-old, severe combined immunodeficient mice (SCID beige) obtained from Charles River (Hollister, CA). Treatment was initiated when mean tumor volume reached 250−300 mm^3. For pharmacodynamic studies, mice were administered a single oral dose of compound in 0.5% methylceullulose/0.2% Tween-80

(MCT). At 1, 4, 8, and 24 h after dosing, mice were euthanized according to IACUC guidelines and tumor samples were harvested and snap frozen on dry ice or fixed in 10% neutral buffered formalin. Tris lysis buffer containing 150 mM NaCl, 20 mM Tris PH 7.5, 1 mM EDTA, 1 mM EGTA, 1% Triton X-100 supplemented with phosphatase and protease inhibitors (Sigma), 1 mM NaF, and 1 mM PMSF was added to frozen tumor biopsies. Tumors were dissociated with a small pestle (Konte Glass Company, Vineland, NJ), sonicated briefly on ice, and centrifuged at maximum RPM for 20 min at 4 °C. Then 20 μg of protein from tumor lysates was used to determine phosphorylation status. Samples were assayed in duplicates per manufacturer's protocol for pSTAT5/tSTAT5 (MSD). Plasma samples were obtained by centrifugation, and drug concentrations were determined using liquid chromatography with tandem mass spectrometric detection (LC/MS).

Kinetic Solubility. Compounds were dissolved in DMSO to a concentration of 10 mM. These solutions were diluted into PBS buffer (pH 7.2, composed with NaCl, KCl, Na_2HPO_4, and KH_2PO_4) to a final compound concentration of 100 μM, DMSO concentration of 2%, at pH 7.4. The samples were shaken for 24 h at room temperature, followed by filtration. LC/CLND was used to determine compound concentration in the filtrate, with the concentration calculated by a caffeine calibration curve and the sample's nitrogen content. An internal standard compound was spiked into each sample for accurate quantification.

Thermodynamic Solubility. Compounds were dissolved in DMSO to a concentration of 10 mM, and these solutions were used to make serial dilutions to 2, 20, and 200 μM. A calibration curve for each compound was generated by LC/UV (254 nM) measurement. Solid compound (2 mg) was placed into Whatman UniPrep filter vials with 0.45 mL PBS buffer (pH 6.5). The vials were shaken for 24 h at room temperature and filtered. The samples were diluted 10× with PBS buffer and analyzed by LC/UV, and the solubility calculated by comparison with the calibration curves.

In Vitro Microsome Metabolic Stability. Experiments were carried out as described.[43]

MDCK Permeability. Experiments were carried out as described.[44]

Crystallography. Jak2 JH1 (kinase) domain was prepared, complexed with compound **8**, crystallized, and its molecular structure determined as described as previously described.[45] See Supporting Information Table S2.

■ ASSOCIATED CONTENT

Supporting Information

Mouse pharmacokinetic parameters for selected compounds, X-ray data collection and refinement details, cocrystal structure (2.3 Å) of compound **8** in the active site of the Jak2 kinase with protein surface displayed, and preparation and characterization of compounds **6b–j**, **7d–k**, **9b–c**, **10b–c**, **13b–g**, **14b–e**, **14g–j**, **18c–d**, **19b–d**, **20b–e**, **22b**, and **26b**. This material is available free of charge via the Internet at http://pubs.acs.org.

Accession Codes

PDB ID for the **8**–Jak2 complex: 4HGE.

■ AUTHOR INFORMATION

Corresponding Author

*Phone: 650-467-6671. E-mail: lyssikatos.joseph@gene.com.

Present Addresses

[#]Department of Cell Biology, Novartis, Emeryville, California. [¶]Department of Infectious Disease, MedImmune, Gaithersburg, Maryland.

Notes

The authors declare no competing financial interest.

■ ACKNOWLEDGMENTS

We thank Christopher Hamman, Michael Hayes, and Mengling Wong for assistance with compound purification, Baiwei Lin for conducting kinetic solubility experiments, Sashi Gopaul, Hoa Le, Emile Plise, Savita Ubhayakar, and Jacob Chen for conducting DMPK experiments, and Sarah Hymowitz and Ivan Bosanac for collecting diffraction data. The Advanced Light Source is supported by the Director, Office of Science, Office of Basic Energy Sciences, of the U.S. Department of Energy under contract no. DE-AC02-05CH11231.

■ ABBREVIATIONS USED

CDI, 1,1′-carbonyldiimidazole; Cl, clearance; DIPEA, *N*,*N*-diisopropylethylamine; DMFDMA, 1,1-dimethoxy-*N*,*N*-dimethylmethanamine; ET, essential thrombocytemia; EtOH, ethanol; HATU, 2-(1*H*-7-azabenzotriazol-1-yl)-1,1,3,3-tetramethyluronoium hexafluorophosphate; HBA, hydrogen bond acceptor; HBD, hydrogen bond donor; Jak, Janus kinase; HLM, human liver microsome; HOAc, acetic acid; LE, ligand efficiency; mCPBA, *meta*-chloroperoxybenzoic acid; MDCK, Madin–Darby canine kidney cells; MF, myelofibrosis; MPD, myeloproliferative disorder; MSD, meso scale discovery; NCS, *N*-chlorosuccinimide; PK/PD, pharmacokinetic/pharmakodynamic; PV, polycythemia vera; PyAOP, 7-azabenzotriazol-1-yloxy-tris-(pyrrolidino)phosphonium hexafluorophosphate; SEM, 2-(trimethylsilyl)ethoxymethyl; STAT, signal transducer and activator of transcription; tBuOH, *tert*-butanol; TDI, time-dependent inhibition; TFA, trifluoroacetic acid; THF, tetrahydrofuran

■ REFERENCES

(1) Yamaoka, K.; Saharinen, P.; Pesu, M.; Holt, V. E., III; Silvennoinen, O.; O'Shea, J. J. The Janus kinases (Jaks). *Genome Biol.* **2004**, *5*, 253.

(2) (a) Aaronson, D. S.; Horvath, C. M. A road map for those who don't know JAK-STAT. *Science* **2002**, *296*, 1653–1655. (b) Kisseleva, T.; Bhattacharya, S.; Braunstein, J.; Schindler, C. W. Signaling through the JAK/STAT pathway, recent advances and future challenges. *Gene* **2002**, *285*, 1–24. (c) O'Shea, J. J.; Gadina, M.; Schreiber, R. D. Cytokine signaling in 2002: new surprises in the Jak/Stat pathway. *Cell* **2002**, *109* (Suppl), S121–S131. (d) Heinrich, P. C.; Behrmann, I.; Haan, S.; Hermanns, H. M.; Muller-Newen, G.; Schaper, F. Principles of interleukin (IL)-6-type cytokine signalling and its regulation. *Biochem. J.* **2003**, *374*, 1–20.

(3) (a) Baxter, E. J.; Scott, L. M.; Campbell, P. J.; East, C.; Fourouclas, N.; Swanton, S.; Vassiliou, G. S.; Bench, A. J.; Boyd, E. M.; Curtin, N.; Scott, M. A.; Erber, W. N.; Green, A. R. Acquired mutation of the tyrosine kinase JAK2 in human myeloproliferative disorders. *Lancet* **2005**, *365*, 1054–1061. (b) James, C.; Ugo, V.; Le Couedic, J.-P.; Staerk, J.; Delhommeau, F.; Lacout, C.; Garcon, L.; Raslova, H.; Berger, R.; Bennaceur-Griscelli, A.; Villeval, J. L.; Constantinescu, S. N.; Casadevall, N.; Vainchenker, W. A unique clonal JAK2 mutation leading to constitutive signaling causes polycythaemia vera. *Nature* **2005**, *434*, 1144–1148. (c) Kralovics, R.; Passamonti, F.; Buser, A. S.; Teo, S.-S.; Tiedt, R.; Passweg, J. R.; Tichelli, A.; Cazzola, M.; Skoda, R. C. A gain-of-function mutation of JAK2 in myeloproliferative disorders. *New Engl. J. Med.* **2005**, *352*, 1779–1790. (d) Levine, R. L.; Wadleigh, M.; Cools, J.; Ebert, B. L.; Wernig, G.; Huntly, B. J.; Boggon, T. J.; Wlodarska, I.; Clark, J. J.; Moore, S.; Adelsperger, J.; Koo, S.; Lee, J. C.; Gabriel, S.; Mercher, T.; D'Andrea, A.; Frohling, S.; Dohner, K.; Marynen, P.; Vandenberghe, P.; Mesa, R. A.; Tefferi, A.; Griffin, J. D.; Eck, M. J.; Sellers, W. R.; Meyerson, M.; Golub, T. R.; Lee, S. J.; Gilliland, D. G. Activating mutation in the tyrosine kinase JAK2 in polycythemia vera essential thrombocythemia, and myeloid metaplasia with myelofibrosis. *Cancer Cell* **2005**, *7*, 387–397.

(e) Zhao, R.; Xing, S.; Li, Z.; Fu, X.; Li, Q.; Krantz, S. B.; Zhao, Z. J. Identification of an acquired JAK2 mutation in polycythemia vera. *J. Biol. Chem.* **2005**, *280*, 22788−22792. (f) Levine, R. L.; Pardanani, A.; Tefferi, A.; Gilliland, D. G. Role of JAK2 in the pathogenesis and therapy of myeloproliferative disorders. *Nature Rev. Cancer* **2007**, *7*, 673−683.

(4) Campbell, P. J.; Green, A. R. The Myeloproliferative Disorders. *New Engl. J. Med.* **2006**, *355*, 2452−2466.

(5) James, C.; Ugo, V.; Casadevall, N.; Constantinescu, S. N.; Vainchenker, W. A JAK2 mutation in myeloproliferative disorders: pathogenesis and therapeutic and scientific prospect. *Trends Mol. Med.* **2005**, *11*, 546−554.

(6) Wernig, G.; Kharas, M. G.; Okabe, R.; Moore, S. A.; Leeman, D. S.; Cullen, D. E.; Gozo, M.; McDowell, E. P.; Levine, R. L.; Doukas, J.; Mak, C. C.; Noronha, G.; Martin, M.; Ko, Y. D.; Lee, B. H.; Soll, R. M.; Tefferi, A.; Hood, J. D.; Gilliland, D. G. Efficacy of TG101348, a selective JAK2 inhibitor, in treatment of a murine model of JAK2V617F-induced polycythemia vera. *Cancer Cell* **2008**, *13*, 311−320.

(7) Hart, S.; Goh, K. C.; Novotny-Diermayr, V.; Hu, C. Y.; Hentze, H.; Tan, Y. C.; Madan, B.; Amalini, C.; Loh, Y. K.; Ong, L. C.; William, A. D.; Lee, A.; Poulsen, A.; Jayaraman, R.; Ong, K. H.; Ethirajulu, K.; Dymock, B. W.; Wood, J. W. SB1518, a novel macrocyclic pyrimidine-based JAK2 inhibitor for the treatment of myeloid and lymphoid malignancies. *Leukemia* **2011**, *25*, 1751−1759.

(8) Ionnidis, S.; Lamb, M. L.; Wang, T.; Almeida, L.; Block, M. H.; Davies, A. M.; Peng, B.; Su, M.; Zhang, H.-J.; Hoffman, E.; Rivard, C.; Green, I.; Howard, T.; Pollard, H.; Read, J.; Alimzhanov, M.; Bebernitz, G.; Bell, K.; Ye, M.; Huszar, D.; Zinda, M. Discovery of 5-Chloro-*N*2-[(1*S*)-1-(5-fluoropyrimidin-2-yl)ethyl]-*N*4-(5-methyl-1*H*-pyrazol-3-yl)-pyrimidine-2,4-diamine (AZD1480) as a Novel Inhibitor of the Jak/Stat Pathway. *J. Med. Chem.* **2011**, *54*, 262−276.

(9) Burkholder, T. P.; Clayton, J. R.; Ma, L. Amino pyrazole compound. U.S. Pat. Appl. Publ. US 20100152181 A1 20100617; CAN 153:97762, AN 2010:753991.201, 2010

(10) (a) Burns, C. J.; Bourke, D. G.; Andrau, L.; Bu, X.; Charman, S. A.; Donohue, A. C.; Fantino, E.; Farrugia, M.; Feutrill, J. T.; Joffe, M.; Kling, M. R.; Kurek, M.; Nero, T. L.; Nguyen, T.; Palmer, J. T.; Phillips, I.; Shakleford, D. M.; Sikanyik, H.; Styles, M.; Su, S.; Treutlein, H.; Zeng, J.; Wilks, A. F. Phenylaminopyrimidines as inhibitors of Janus kinases (JAKs). *Bioorg. Med. Chem. Lett.* **2009**, *19*, 5887−5882. (b) Tyner, J. W.; Bumm, T. G.; Deininger, J.; Wood, L.; Aichberger, K. J.; Loriaux, M. M.; Druker, B. J.; Burns, C. J.; Fantino, E.; Deininger, M. W. CYT387, a novel JAK2 inhibitor, induces hematologic responses and normalizes inflammatory cytokines in murine myeloproliferative neoplasms. *Blood* **2010**, *115*, 5232−5240.

(11) Verstovsek, S.; Kantarjian, H.; Mesa, R. A.; Pardanani, A. D.; Cortes-Franco, J.; Thomas, D. A.; Estrov, Z.; Fridman, J. S.; Bradley, E. C.; Erickson-Viitanen, S.; Vaddi, K.; Levy, R.; Tefferi, A. Safety and efficacy of INCB018424, a JAK1 and JAK2 inhibitor, in myelofibrosis. *New Engl. J. Med.* **2010**, *363*, 1117−1127.

(12) Quintas-Cardama, A.; Vaddi, K.; Liu, P.; Manshouri, T.; Li, J.; Scherle, P. A.; Caulder, E.; Wen, X.; Li, Y.; Waeltz, P.; Rupar, M.; Burn, T.; Lo, Y.; Kelley, J.; Covington, M.; Shepard, S.; Rodgers, J. D.; Haley, P.; Kantarjian, J.; Fridman, J. S.; Verstovsek, S. Preclinical characterization of the selective JAK1/2 inhibitor INCB018424: therapeutic implications for the treatment of myeloproliferative neoplasms. *Blood* **2010**, *115*, 3109−3117.

(13) (a) Macchi, P.; Villa, A.; Giliani, S.; Sacco, M. G.; Frattini, A.; Porta, F.; Ugazio, A. G.; Johnston, J. A.; Candotti, F.; O'Shea, J. J.; Vezzoni, P.; Notarangelo, L. D. Mutations of Jak-3 gene in patients with autosomal severe combined immune deficiency (SCID). *Nature* **1995**, *377*, 65−68. (b) Russell, S. M.; Tayebi, N.; Nakajima, H.; Riedy, M. C.; Roberts, J. L.; Aman, M. J.; Migone, T. S.; Noguchi, M.; Markert, M. L.; Buckley, R. H.; O'Shea, J. J.; Leonard, W. J. Mutation of Jak3 in a patient with SCID: essential role of Jak3 in lymphoid development. *Science* **1995**, *270*, 797−800. (c) Rodig, S. J.; Meraz, M. A.; White, J. M.; Lampe, P. A.; Riley, J. K.; Arthur, C. D.; King, K. L.; Sheehan, K. C.; Yin, L.; Pennica, D.; Johnson, E. M., Jr.; Schreiber, R. D. Disruption of the Jak1 gene demonstrates obligatory and nonredundant roles of the Jaks in cytokine-induced biologic responses. *Cell* **1998**, *93*, 373−383.

(14) The prescribing information for ruxolitinib (Jakafi) includes: "Active serious infections should have resolved before starting therapy with Jakafi. Physicians should carefully observe patients receiving Jakafi for signs and symptoms of infection and initiate appropriate treatment promptly."

(15) Hopkins, A. L.; Groom, C. R.; Alex, A. Ligand efficiency: a useful metric for lead selection. *Drug Discovery Today* **2004**, *9*, 430−431.

(16) Keseru, G. M.; Makara, G. M. The influence of lead discovery strategies on the properties of drug candidates. *Nature Rev. Drug Discovery* **2009**, *8*, 203−212.

(17) Cruciani, G.; Crivori, P.; Carrupt, P.-A.; Testa, B. Molecular fields in quantitative structure-permeation relationships: the VolSurf approach. *J. Mol. Struct. (THEOCHEM)* **2000**, *503*, 17−30.

(18) Gavrin, L. K.; Lee, A.; Provencher, B. A.; Massefski, W. W.; Huhn, S. D.; Ciszewski, G. M.; Cole, D. C.; McKew, J. C. Synthesis of pyrazolo[1,5-alpha]pyrimidinone regioisomers. *J. Org. Chem.* **2007**, *72*, 1043−1046.

(19) Miyaura, N.; Suzuki, A. Palladium-Catalyzed Cross-Coupling Reactions of Organoboron Compounds. *Chem. Rev.* **1995**, *95*, 2457−2483.

(20) Chen, C.; Wilcoxen, K.; McCarthy, J. R. A convenient one-pot synthesis of 4-amino-3-arylpyrazoles from alpha-phthaloylaminoacetophenones. *Tetrahedron Lett.* **1998**, *39*, 8229−8232.

(21) Clay, R. J.; Collom, T. A.; Karrick, G. L.; Wemple, J. A safe, economical method for the preparation of beta-oxo esters. *Synthesis* **1993**, 290−292.

(22) Shioiri, T.; Ninomiya, K.; Yamada, S. Diphenylphosphoryl azide: a new convenient reagent for a modified Curtius reaction and for the peptide synthesis. *J. Am. Chem. Soc.* **1972**, *94*, 6203−6205.

(23) Identity of regioisomers definitevely assigned via ^{1}H NMR nuclear Overhauser effect.

(24) Goikhman, R.; Jacques, T. L.; Sames, D. C−H bonds as ubiquitous functionality: a general approach to complex arylated pyrazoles via sequential regioselective *C*-arylation and *N*-alkylation enabled by SEM-group transposition. *J. Am. Chem. Soc.* **2009**, *131*, 3042−3048.

(25) Invitrogen Selectscreen Kinase Profiling service. Five kinases (DAPK1, Ros, TRKA, TRKB, TRKC) were inhibited greater than 50% by 7a at a compound concentration of 200 nM, a concentration approximately 100-fold higher than the Jak2 K_i.

(26) Mouse pharmacokinetic data is available in tabulated form as Supporting Information, Table S1.

(27) Ritchie, T. J.; MacDonald, S. J.; Young, R. J.; Pickett, S. D. The impact of aromatic ring count on compound developability: further insights by examining carbo- and hetero-aromatic and -aliphatic ring types. *Drug. Discovery Today* **2011**, *16*, 164−171.

(28) (a) Jiang, H.; Leger, J.-M.; Dolian, C.; Guionneau, P.; Huc, I. Aromatic δ-peptides: design, synthesis and structural studies of helical, quinoline-derived oligoamide foldamers. *Tetrahedron* **2003**, *59*, 8365−8374. (b) Pierce, A. C.; ter Haar, E.; Binch, H. M.; Kay, D. P.; Patel, S. R.; Li, P. CH···O and CH···N hydrogen bonds in ligand design: a novel quinazolin-4-ylthiazol-2-ylamine protein kinase inhibitor. *J. Med. Chem.* **2005**, *48*, 1278−1281. (c) Yoshikawa, K.; Kobayashi, S.; Nakamoto, Y.; Haginoya, N.; Komoriya, S.; Yoshino, T.; Nagata, T.; Mochizuki, A.; Watanabe, K.; Suzuki, M.; Kanno, H.; Ohta, T. Design, synthesis, and SAR of *cis*-1,2-diaminocyclohexane derivatives as potent factor Xa inhibitors. Part II: exploration of 6−6 fused rings as alternative S1 moieties. *Bioorg. Med. Chem.* **2009**, *17*, 8221−8233. (d) Bissantz, C.; Kuhn, B.; Stahl, M. A medicinal chemist's guide to molecular interactions. *J. Med. Chem.* **2010**, *53*, 5061−5084. (e) Shimizu, H.; Tanaka, S.; Toki, T.; Yasumatsu, I.; Akimoto, T.; Morishita, K.; Yamasaki, T.; Yasukochi, T.; Iimura, S. Discovery of imidazo[1,2-*b*]pyridazine derivatives as IKKβ inhibitors. Part 1: Hit-to-lead study and structure−activity relationship. *Bioorg. Med. Chem. Lett.* **2010**, *20*, 5113−5118. (f) Dubey, R.; Lim, D. Weak interactions: a

versatile role in aromatic compounds. *Curr. Org. Chem.* **2011**, *15*, 2072−2081.

(29) Amino acid differences between Jak2 and other family members are as follows. Jak3 amino acid:Jak2-Gln832:Ser, Met865:Leu, Tyr934:Ser, Ser936:Cys, Lys943:Arg, Gly993:Arg. Tyk2 amino acid:Jak2-Lys857:Glu, Val911:Ile, Leu932:Val, Tyr934:Leu, Lys943:Arg.

(30) (a) Ju, C.; Uetrecht, J. P. Mechanism of idiosyncratic drug reactions: reactive metabolite formation, protein binding and the regulation of the immune system. *Curr. Drug Metab.* **2002**, *3*, 367−377. (b) Evans, D. C.; Watt, A. P.; Nicoll-Griffith, D. A.; Baillie, T. A. Drug−protein adducts: an industry perspective on minimizing the potential for drug bioactivation in drug discovery and development. *Chem. Res. Toxicol.* **2004**, *17*, 3−16. (c) Soglia, J. R.; Harriman, S. P.; Zhao, S.; Barberia, J.; Cole, M. J.; Boyd, J. G.; Contillo, L. G. The development of a higher throughput reactive intermediate screening assay incorporating micro-bore liquid chromatography-micro-electrospray ionization-tandem mass spectrometry and glutathione ethyl ester as an in vitro conjugating agent. *J. Pharm. Biomed. Anal.* **2004**, *36*, 105−116. (d) Kalgutkar, A. S.; Gardner, I.; Obach, R. S.; Shaffer, C. L.; Callegari, E.; Henne, K. R.; Mutlib, A. E.; Dalvie, D. K.; Lee, J. S.; Nakai, Y.; O'Donnell, J. P.; Boer, J.; Harriman, S. P. A comprehensive listing of bioactivation pathways of organic functional groups. *Curr. Drug. Metab.* **2005**, *6*, 161−225.

(31) Blagg, J. Structure−activity relationships for in vitro and in vivo toxicity. *Annu. Rep. Med. Chem.* **2006**, *41*, 353−368.

(32) (a) Milletti, F.; Storchi, L.; Sforna, G.; Cruciani, G. New and original pK_a prediction method using grid molecular interaction fields. *J. Chem. Inf. Model.* **2007**, *47*, 2172−2181. (b) Milletti, F.; Storchi, L.; Goracci, L.; Bendels, S.; Wagner, B.; Kansy, M.; Cruciani, G. Extending pK_a prediction accuracy: high-throughput pK_a measurements to understand pK_a modulation of new chemical series. *Eur. J. Med. Chem.* **2010**, *45*, 4270−4279.

(33) van De Waterbeemd, H.; Smith, D. A.; Beaumont, K.; Walker, D. K. Property-based design: optimization of drug absorption and pharmacokinetics. *J. Med. Chem.* **2001**, *44*, 1313−1333.

(34) Laurence, C.; Brameld, K. A.; Graton, J.; Le Questel, J. Y.; Renault, E. The pK(BHX) database: toward a better understanding of hydrogen-bond basicity for medicinal chemists. *J. Med. Chem.* **2009**, *52*, 4073−4086.

(35) Testa, B.; Jenner, P. Inhibitors of Cytochrome P-450s and their mechanism of action. *Drug Metab. Rev.* **1981**, *12*, 1−117.

(36) (a) Iwaoka, M.; Takemoto, S.; Tomoda, S. Statistical and theoretical investigations on the directionality of nonbonded S···O interactions. Implications for molecular design and protein engineering. *J. Am. Chem. Soc.* **2002**, *124*, 10613−10620. (b) Haginoya, N.; Kobayashi, S.; Komoriya, S.; Yoshino, T.; Suzuki, M.; Shimada, T.; Watanabe, K.; Hirokawa, Y.; Furugori, T.; Nagahara, T. Synthesis and conformational analysis of a non-amidine factor Xa inhibitor that incorporates 5-methyl-4,5,6,7-tetrahydrothiazolo[5,4-*c*]pyridine as S4 binding element. *J. Med. Chem.* **2004**, *47*, 5167−5182. (c) Nettekoven, M.; Guba, W.; Neidhart, W.; Mattei, P.; Pflieger, P.; Roche, O.; Taylor, S. Isomeric thiazole derivatives as ligands for the neuropeptide Y5 receptor. *Bioorg. Med. Chem. Lett.* **2005**, *15*, 3446−3449. (d) Sugiyama, H.; Yoshida, M.; Mori, K.; Kawamoto, T.; Sogabe, S.; Takagi, T.; Oki, H.; Tanaka, T.; Kimura, H.; Ikeura, Y. Synthesis and structure−activity relationship studies of benzothieno[3,2-*b*]furan derivatives as a novel class of IKKbeta inhibitors. *Chem. Pharm. Bull.* **2007**, *55*, 613−624.

(37) Lovering, F.; Bikker, J.; Humblet, C. Escape from flatland: increasing saturation as an approach to improving clinical success. *J. Med. Chem.* **2009**, *52*, 6752−6756.

(38) Good agreement was observed between the pSTAT5 SET2 MSD format used for compounds in Tables 1 and 2 and the pSTAT5 TF1+EPO MSD format used for compounds in Table 4. Compound **7j** was assessed in both formats, with IC_{50} = 3.9 nM in the SET2 format as compared with IC_{50} = 7.4 nM in the TF1+EPO format. See the Experimental Section for details on both cell assays.

(39) TDI was observed sporadically in compounds in this chemical series with no clear SAR.

(40) Invitrogen Selectscreen Kinase Profiling service. IC_{50}s: Fyn 4.97 μM, Ros 15.2 μM, TrkA 3.97 μM, TrkB 5.38 μM, TrkC 1.3 μM.

(41) Lee, L.; Berry, M.; Zhou, A.; Rawson, T.; Hanan, E.; Li, J.; Bir Kohli, P.; Barrett, K.; Chang, C.; Chen, J.; Ubhayakar, S.; Siu, M.; Kenny, J.; Johnson, A.; Van Abbema, A.; Blair, W.; Ghilardi, N.; Sampath, D. Development and validation of a novel acute myeloid leukemia xenograft model that is dependent on the JAK2 V617F mutation for growth in vivo. *Mol. Cancer Ther.* **2009**, *8*, A20 GNE-372 refers to compound **7j**..

(42) (a) Morrison, J. F. Kinetics of the reversible inhibition of enzyme-catalysed reactions by tight-binding inhibitors. *Biochim. Biophys. Acta* **1969**, *185*, 269−286. (b) Williams, J. W.; Morrison, J. F. The kinetics of reversible tight-binding inhibition. *Methods Enzymol.* **1979**, *63*, 437−467.

(43) Halladay, J. S.; Wong, S.; Jaffer, S. M.; Sinhababu, A. K.; Khojasteh-Bakht, S. C. Metabolic stability screen for drug discovery using cassette analysis and column switching. *Drug. Metab. Lett.* **2007**, *1*, 67−72.

(44) (a) Irvine, J. D.; Takahashi, L.; Lockhart, K.; Cheong, J.; Tolan, J. W.; Selick, H. E.; Grove, J. R. MDCK (Madin−Darby canine kidney) cells: A tool for membrane permeability screening. *J. Pharm. Sci.* **1999**, *88*, 28−33. (b) Plise, E.; Sindelar, E.; Duck, B.; Cheong, J.; Sodhi, J.; Salphati, L. Fully Automated 24-Well Madlin−Darby Canine Kidney (MDCK) Permeability Assay Utilizing the Hamilton Microlab Star Liquid Handling Platform. *AAPS Annu/ Meet.* **2009**. AAPS Abstract: http://www.aapsj.org/abstracts/AM_2009/AAPS2009-001769.PDF.

(45) (a) Kulagowski, J. J.; Blair, W.; Bull, R. J.; Chang, C.; Deshmukh, G.; Dyke, H. J.; Eigenbrot, C.; Ghilardi, N.; Gibbons, P.; Harrison, T. K.; Hewitt, P. R.; Liimatta, M.; Hurley, C. A.; Johnson, A.; Johnson, T.; Kenny, J.; Kohli, P. B.; Maxey, R. J.; Mendonca, R.; Mortara, K.; Murray, J.; Narukulla, R.; Shia, S.; Steffek, M.; Ubhayakar, S.; Ultsch, M.; van Abbema, A.; Ward, S. I.; Waszkowycz, B; Zak, M. Identification of imidazo-pyrrolopyridines as novel and potent JAK1 inhibitors. *J. Med. Chem.* **2012**, *55*, 5901−5921. (b) Zak, M.; Mendonca, R.; Balazs, M.; Barrett, K.; Bergeron, P.; Blair, W. S.; Chang, C.; Deshmukh, G.; DeVoss, J.; Dragovich, P. S.; Eigenbrot, C.; Ghilardi, N.; Gibbons, P.; Gradl, S.; Hamman, C.; Hanan, E.; Harstad, E.; Hewitt, P. R.; Hurley, C. A.; Jin, T.; Johnson, A.; Johnson, T.; Kenny, J. R.; Koehler, M. F. T.; Kohli, P. B.; Kulagowski, J.; Labadie, S.; Liao, J.; Liimatta, M.; Lin, Z.; Lupardus, P. J.; Maxey, R. J.; Murray, J. M.; Pulk, R.; Rodriguez, M.; Savage, S.; Shia, S.; Steffek, M.; Ubhayakar, S.; Ultsch, M.; Van-Abbema, A.; Ward, S.; Xiao, L.; Xiao, Y. Discovery and optimization of C-2 methyl imidazo-pyrrolopyridines as potent and orally bioavailable JAK1 inhibitors with selectivity over JAK2. *J. Med. Chem.* **2012**, *55*, 6176−6193.